EXPERIMENTAL STUDY OF STRIPLINE–FED SLOT RADIATORS FOR ARRAY APPLICATIONS

A Thesis Submitted

in Partial Fulfillment of the Requirements

for the Degree of

Master of Technology

by

Major Sanjeev Govila

to the

DEPARTMENT OF ELECTRICAL ENGINEERING

INDIAN INSTITUTE OF TECHNOLOGY, KANPUR

April 1994

Certificate

It is certified that the work contained in the thesis entitled **EXPERIMENTAL STUDY OF STRIPLINE-FED SLOT RADIATORS FOR ARRAY APPLICATIONS**, by Major Sanjeev Govila, has been carried out under my supervision and that this work has not been submitted elsewhere for a degree.

29-3-
April 1994

M Sachidananda

Dr M Sachidananda

Professor

Department of Electrical Engineering

I.I.T. Kanpur

EE-1994-M-GOV-EXP

Abstract

In this thesis, an attempt has been made to fabricate and experimentally study two structures in stripline-fed slot arrays for suppression of parallel plate guide mode. The two structures , namely , cavity-backed stripline-fed slot and stripline-fed slot pair have been proposed , fabricated , tested and their various characteristic curves have been plotted and experimentally studied to forward meaningful conclusions and suggestions for further work.

To

MY PARENTS

Acknowledgements

Lion's share for the successful completion of this thesis work goes to my guide, Dr. M. Sachidananda, whose attention to details, orderliness, professional knowledge and, above all, easy accessibility, have always wondered me.

I am indebted to Apu Sivadasa, Harish and, now NRI, Srikant for their ever helpful attitudes.

I also thank the Department of Electrical Engineering and the Advanced Centre for Electronic Systems for all the facilities provided to me and for a very cordial and enjoyable working atmosphere.

My sincere thanks also go out to all my defence friends who helped make my stay at IIT, Kanpur an ever memorable one.

I give all my regards to all the good samaritans at the Computer Centre who came forward at the times of distress and helped me beyond my frontiers of knowledge.

Last, but not the least, I would unhesistingly attribute a large part of my success to my wife *Bindu* and to my dear daughter *Shelly* for their kind understanding, standing up to all my idiosyncracies and offerring me an ever cheerful atmosphere in the house.

Major Sanjeev Govila

Contents

1 Introduction 1

1.1 General 1

1.2 Literature survey 2

2 Suppression of Parallel Plate Guide Mode in Slot Arrays 7

2.1 Introduction 7

2.2 Conventional methods 7

2.3 Cavity backed slot 8

2.4 Cancellation using slot pair 10

2.5 Scope of this study 11

3 Cavity-backed Stripline-fed Slot Antenna 12

3.1 Introduction 12

3.2 Design details 12

3.2.1 Cavity design considerations 12

3.2.2 Stripline feed and slot design considerations 14

3.3 Fabrication details 15

3.4 Measurement setup and procedure 16

3.4.1 Introduction 16

3.4.2 Measurement of the S_{11} characteristics 17

3.4.3 Generation of radiation plot 18

3.5 Results 20

3.6 Observation 21

3.7 Conclusion 27

4 Suppression of Parallel Plate Guide Mode Using a Slot Pair **31**

4.1 Introduction 31

4.2 Design considerations 31

4.2.1 Self impedance of centre-fed cylinderical dipole 32

4.2.2 Mutual admittance of centre-fed cylinderical dipoles 34

4.2.3 Active impedance of centre-fed rectangular slots 35

4.3 Fabrication details 37

4.4 Measurement setup and procedure 38

4.5 Results 40

4.6 Observations 41

4.7 Conclusion 56

5 Conclusion **57**

List of Figures

1.1 Layout showing radiating slots (solid), stripline feed (dashed) and the pin curtain 5

1.2 Slot array with internal cavities 6

2.1 Pin curtain in a large slot array 8

2.2 Cavity backed slot with a stripline feed 9

2.3 Cancellation using slot pair 10

3.1 Stripline-fed cavity-backed circular slot 13

3.2 Rectangular stripline-fed cavity-backed slot 16

3.3 Outline of the rubylith cut for the etching 17

3.4 Experimental setup for measurement of S_{11} characteristics 18

3.5 Experimental setup for the radiation plot 19

3.6 S_{11} characteristics : 0.0 and 4.72 mm cavities 22

3.7 S_{11} characteristics : 5.97 and 10.27 mm cavities 23

3.8 S_{11} characteristics : 12.92 and 15.2 mm cavities 24

3.9 Comparison of S_{11} characteristics of all cavities with foil 25

3.10 Comparison of S_{11} characteristics of all cavities without foil 26

3.11 Radiation plot for a shorted cavity 28

3.12 Radiation plot for a 5.97 mm cavity 29

4.1 Two parallel cylinderical dipoles 34
4.2 Design of the stripline-fed slot pair 39
4.3 Experimental setup for the stripline-fed slot pair 40
4.4 Curves for Offset=0.5mm and Slot length=13.6mm. 43
4.5 Curves for Offset=0.9mm and Slot length=14.1mm 44
4.6 Curves for Offset=1.0mm and Slot length=14.2mm 45
4.7 Curves for Offset=2.0mm and Slot length=14.2 mm 46
4.8 Curves for Offset=3.0mm and Slot length=14.2mm 47
4.9 Curves for Offset=4.0mm and Slot length=14.2 mm 48
4.10 Curves for Offset=4.5mm and Slot length=14.2mm 49
4.11 Curves for Offset=4.5mm and Slot length=15.2mm 50
4.12 Curves for Offset=2.0mm and Slot length=15.2mm 51
4.13 Curves of S_{11} characteristics for comparison 52
4.14 Main lobe radiation pattern at selected settings 53
4.15 Side radiation patterns for selected settings 55

Chapter 1

Introduction

1.1 General

Prior to the advent of printed antennas, slot radiators in various configuration in waveguides had become quite popular. These configurations had many practical applications as single radiating elements but were also used extensively in arrays. Such antenna applications involving slots unify the feeding and radiating structures by placing the slots in one of the walls of a rectangular waveguide. This insures a non-radiating transmission line, permits precise machining of the slots, and provides a mechanically rigid structure. Usually the slots are arranged in arrays, which complicate the feeding because of mutual coupling.

With the use of printed technology in fabricating antennas, slot radiators in microstrips, striplines etc. started finding more favour due to the advantages of savings in cost, size and weight and having a low profile.

1.2 Literature survey

Several authors [1], [2] have reported about antennas utilizing microstrip lines since early 1950s where several types of array patterns were printed on the substrates of microstrip lines. Around 1954, slot antennas utilising triplate striplines have also been reported by Oliner [3] and Sommers [4].

Robert W. Breithaupt [5] plotted frequency-independent curves for calculating the conductance of offset series slots in striplines for 50 Ω characteristic impedance and three common ground plane spacings. He also gave an experimental verification for a particular case.

Y. Yoshimura in [6] treated a microstrip line slot antenna experimentally at X-band frequency. He measured the input impedance of the slots for various geometries and the radiation pattern for matched slots. After testing the dependance of input impedance and radiation patterns on the slot-to-reflector spacing, he designed and fabricated a two dimensional X-band Dolph-Chebychev slot array antenna.

Oltman [7] describes a novel antenna element in which the element consists of an unbroken strip dipole which is electromagnetically coupled to a microstrip feed line that occupies some of the region under the dipole. Coupling is varied in amplitude and phase by offsetting the dipole either transversly or longitudinally relative to the microstrip and by changing the length of the dipole.

D. A. Heubner [8], one of the Ottman's co-workers at Hughes Aircraft Company, reported on the performance of a planar microstrip dipole array using Ottman's element . Excitation of the dipoles was accomplished by a corporate feed using equal power dividers and relying on density tapering of the elements to achieve the desired aperture distribution. The intended sidelobe level was not achieved which

was ascribed to the neglected mutual coupling.

R. S. Elliott and George J. Stern [9] extended this work and developed a theory to explain the behavior of planar arrays of microstrip dipoles. They obtained relations involving the active input impedances of individual dipoles (thus recognising the effects of mutual coupling) and the radiating currents in the dipoles resulting from a set of impressed voltages.

During the same time, another paper by Pyong K. Park and Robert S. Elliott presented an analytical design method for a collinear longitudinal slot arrays fed by a boxed stripline. It enables determination of the length of each slot in a collinear array and the tilt angle of the strip relative to each slot for a specified aperture distribution and input impedance, in the presence of external mutual coupling.

B. N. Das and K. K. Joshi [11] dealt with the impedance of a radiating slot in the ground plane of a stripline . They have derived an expression for the complex admittance of a radiating slot in the ground plane of a microstrip line from the complex radiated power and the discontinuity in the modal voltage. The complex radiated power is obtained from the angular spectrum of the plane waves.

An analytical design method applicable to linear transverse slot arrays [12] fed by a boxed stripline was developed by Reuven Shavit and Robert S. Elliott. Utilising the method of moments, the fields in the slot are approximated. Then, an array design technique which accounts for the external mutual coupling is presented.

In November 1984, B. N. Das and K. V. S. V. R. Prasad [13] analysed the impedance of a transverse slot in the ground plane of an offset stripline. The result of the analysis are used to compute the variation of slot impedance with strip offset and also with change in position of one of the ground planes.

Ralston S. Robertson and Robert S.Elliott [14] conudcted theoretical and ex-

perimental investigation of transverse slots fed by a boxed stripline, with the strip passing centrally under the slot. They have developed a procedure which permitted the design of arrays of such slots, including the effects of mutual coupling. They have shown that aggrement between theory and experiment are good for both, a single slot and a linear array.

In his paper, Shavit [12] had designed a module in which the strip passed at a right angle under the slot near one of its ends, with the coupling controlled by the distance the strip was in from the end of the slot. The waveguide dimensions were chosen to allow the TE_{10} mode to propagate, thus permitting a reasonable resonant length for the slot. However, successive slots needed to be isolated from each other by the use of transverse pin curtains which only allowed the passage of the TEM mode. The pin curtains also served another purpose. Their position was used to control the resonant length of the slot. As this model was found to be successful, Robertson [14] too used similar pin curtains in his work, as shown in Figure 1.1.

Robert J. Mailloux [15] carried out a detailed analysis of infinite printed slot arrays with dielectric substrates using metallized cavities and excited by delta-function current sources. He showed that an alternative to using pins or plating through holes in the ground planes is using metallic walls between the slot elements to achieve the desired isolation from internal coupling through the parallel plate feed structure. Such walls can be formed by milling the cavities from a metal block, as shown in Figure 1.2.

However whether it be pins, metallized cavities or holes drilled through, there are some practical difficulties when large arrays are being designed. In an array with a large number of slots, driving pins or drilling holes around each slot becomes very laborious and may actually interfere physically with the feed lines *specially if the*

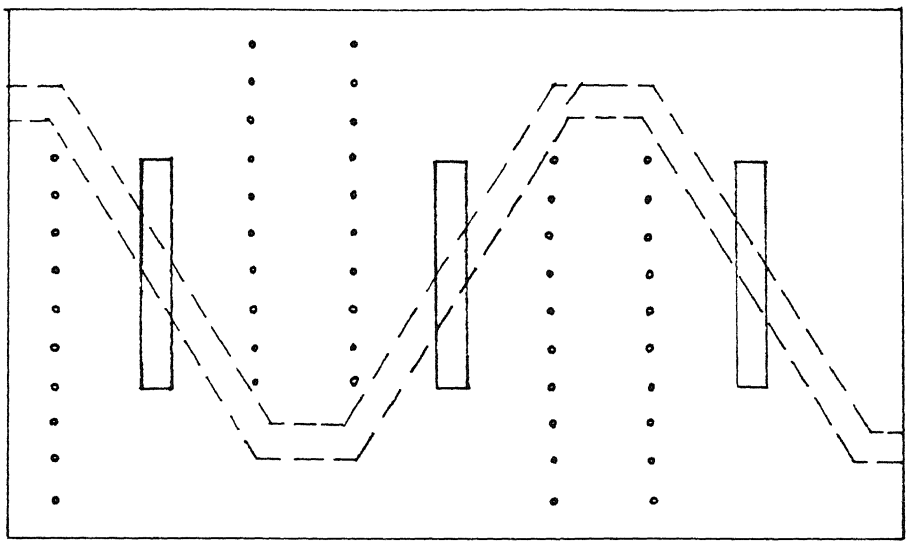

Figure 1.1: Layout showing radiating slots (solid), stripline feed (dashed) and the pin curtain

slots are very near and/or the overall size of the array is small. Similarly, if a corporate feed is used for the printed slots, the metallized cavities would interfere physically with the feed lines.

Thus, it becomes very important to devise ways and means by which a good internal isolation can be provided between adjacent slots in a slot array by suppressing the parallel plate guide mode without a recourse to the conventional methods.

This thesis work attempts to experimentally study two methods for achieving this objective. The two methods have been described in detail, accompanied by sufficient curves to analyse the proposed methods. Finally, a conclusion has been arrived at for further work in the area.

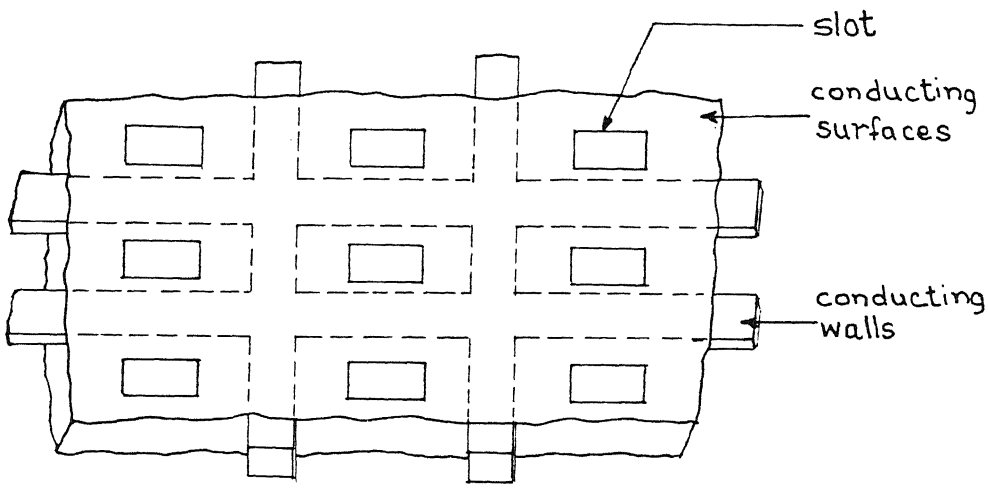

Figure 1.2: Slot array with internal cavities

Chapter 2

Suppression of Parallel Plate Guide Mode in Slot Arrays

2.1 Introduction

It has already been pointed out in the previous chapter that there is a considerable amount of internal coupling in a parallel plate guide mode between adjacent slots in an array. Slot arrays in a stripline substrate are prone to this problem as they also form a parallel plate guide mode internally due to the feed-line structure. Pin curtains, metallized cavities and holes drilled around each slot are the methods which have already been touched upon. Two new methods have been tried out in this thesis work, to be dealt with subsequently.

2.2 Conventional methods

In literature [12], [14] , generally pin curtains seem to be the most widely used method for suppression of the parallel plate guide mode. However, if we visualise a big slot array, specially of small physical dimensions and small distance between adjacent slots, as shown in Figure 2.1, it is very easy to visualise the practical problems

involved indriving through such a large number of shorting pins. Add to this the

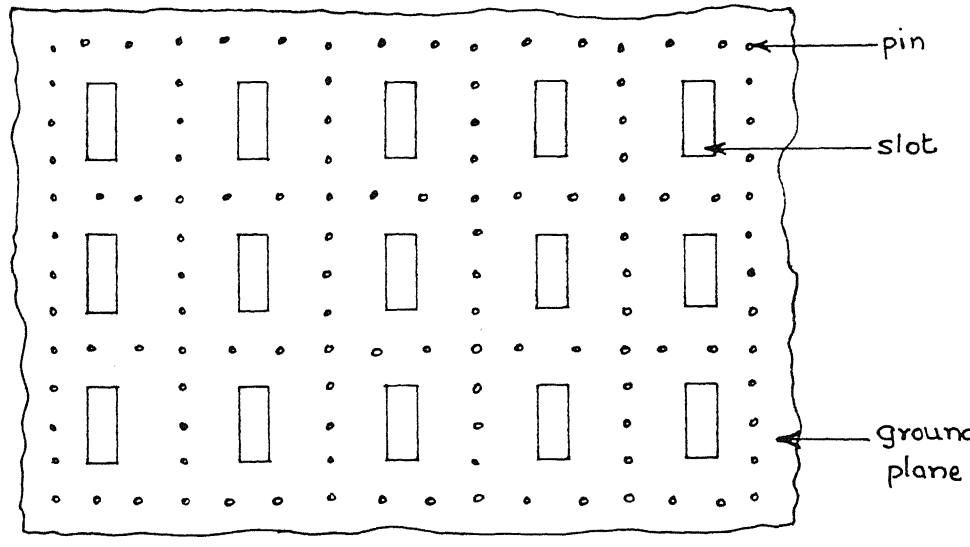

Figure 2.1: Pin curtain in a large slot array

fact that the feeding structure has not been shown in Fig 2.1. Same is the case with metallized cavities and drilled holes. Thus, though these conventional methods have been well analyzed and found to be satisfactory, they have their limitations for certain specific applications.

2.3 Cavity backed slot

This is a new method tried out in this thesis work. Here a slot has been made in the lower ground plane of a stripline and cavity backing given there. An attempt has been made to adjust the dimensions of the cavity in such a way that , at resonance, the field reflected from the cavity effectively cancel out the side radiations emanating from the stripline feed. This is shown in Fig 2.2. Here, the reflected fields from

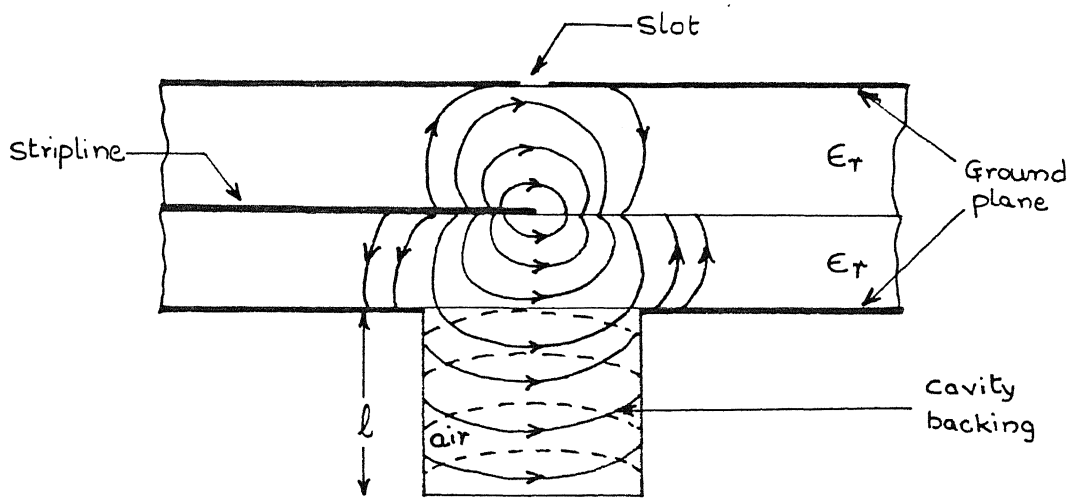

Figure 2.2: Cavity backed slot with a stripline feed

the cavity attempt to cancel out the side radiations and also couple with the slot on the upper ground plane to radiate in the atmosphere. To be able to cancel out the side radiations effectively, there is a need to analyse the fields in this cavity and their interaction with the fields in the parallel plate guide mode . Since there is no literature dealing with this problem and this thesis work is attempting only an experimental study, it was decided to use a waveguide with a sliding short. With the short sliding, the effect of changing cavity dimensions on S_{11} and radiation pattern was noted. The emerging pattern was then studied to arrive at conclusions, as dealt with in Chapter 3.

2.4 Cancellation using slot pair

This is the second method tried out in this thesis work. The basic rationale behind using this method is quite simple as outlined in Fig. 2.3. With the slots exactly $\frac{\lambda_g}{2}$

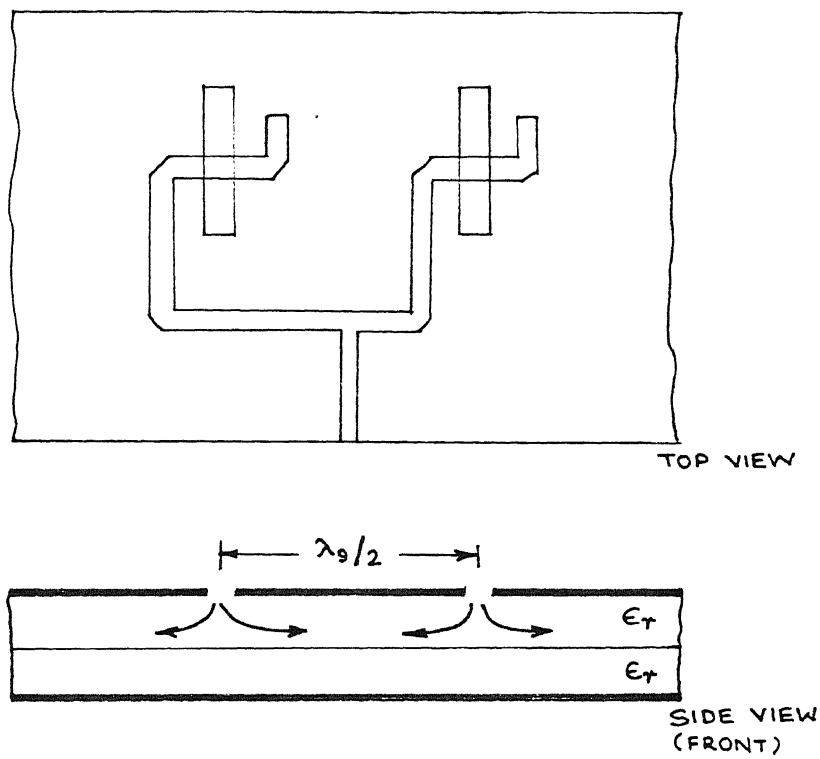

Figure 2.3: Cancellation using slot pair

apart, the side radiations of the parallel plate guide mode would effectively cancel each other out. However, in practice, the designing is not as simple. The mutual coupling of the close slots has to be taken into account while determining their dimensions and spacing. Compared to a cavity backed slot, the slot pair method is compact and easier to fabricate. *Though for each slot an additional slot has to be fabricated,* it is quite easy in printed technology. Chapter 4 of this thesis work deals with this method.

2.5 Scope of this study

This study aims at :—

- Designing, fabricating and doing suitable measurements on a cavity-backed stripline–fed slot so as to plot various curves, studying their relationships and drawing conclusions out of them.

- Repeating the above procedure with a stripline–fed slot pair.

No rigorous analysis has been attempted in this study. Here, only an experimental study has been conducted with the main aim of studying new structures for the suppression of the parallel plate guide mode in stripline–fed slot arrays.

Chapter 3

Cavity-backed Stripline-fed Slot Antenna

3.1 Introduction

There is no literature presently available dealing specifically with a cavity-backed stripline-fed slot. The closest one gets to [16] is a slot antenna in an infinite ground plane with cavity backing. As no rigorous thoretical analysis has been done, the design of the structure fabricated for the purpose of this study has been based on the knowledge of slot antennas with cavity backing and stripline-fed slots. To be able to do a meaningful experimental study, the cavity used has a variable short and the graphs have been plotted at various short settings.

3.2 Design details

3.2.1 Cavity design considerations

It was decided to use a circular cavity as it is easier to mill a circular cavity than a rectangular one on a solid block. The overall setup was visualised to be as in Fig 3.1.

The requirements for the circular waveguide to be used were to be that:—

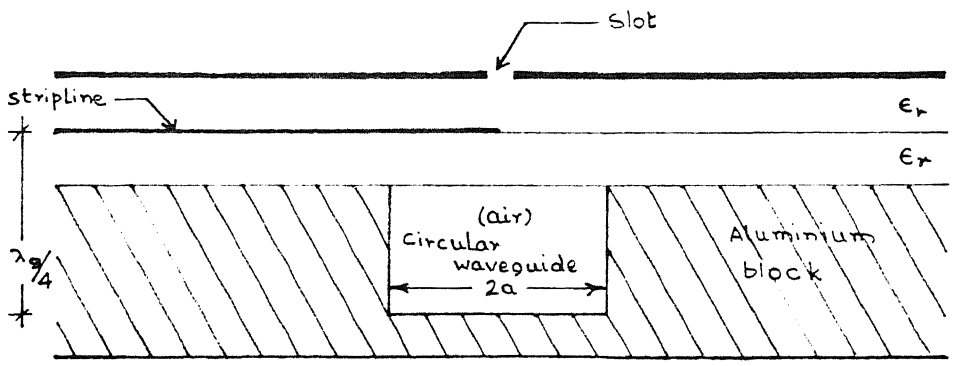

Figure 3.1: Stripline-fed cavity-backed circular slot

1. $\frac{V_g}{V_o} > 0.7$

   where

   V_g = velocity of the waves in the guide and

   V_o = velocity in free space.

2. Only TE_{11} mode should propagate i. e. next higher mode, TM_{01} should not propagate.

Based on these considerations, a computer program was made and for a frequency of 10 GHz, the diameter was calculated to be 2.29 cms. However, then it was found not to be very easy practically to vary the length of the waveguide. The need for the length to be variable was felt because, as can be seen, the whole setup was quite complicated with many transitions taking place. Without the help of a rigorous theoretical analysis, it is difficult to visualise how the setup would exactly behave. It, thus, is difficult to calculate the exact length of the circular waveguide for resonance.

Finally, a commercially available rectangular waveguide based micrometer-type sliding short was used. This equipment is normally used for mirowave experiments

In laboratories.

It was found that this waveguide did not have a flat surface at the short. There were flanges. Thus, there was a need to establish a zero setting. For this purpose, its propagation constant, β was found out by the formula

$$\beta = \sqrt{\omega^2\mu\epsilon - (m\pi/a)^2 - (n\pi/b)^2} \tag{3.1}$$

where

β = propagation constant

$\omega = 2\pi f$ where f = freq of operation

m , n = mode of operation

a ,b = length, breadth of the waveguide

μ = permeability of the medium

ϵ = permittivity of the medium

Then using the network analyser 8410A (Hewlett-Packard), the phase-shift at zero micro-meter reading was found out.The equivalent electrical length was then found out using the calculated value of β.

3.2.2 Stripline feed and slot design considerations

Using a substrate RT/Duroid with $\epsilon_r = 2.2$ and thickness of 0.794 mm, the width of a stripline of $Z = 50\Omega$ was found out to be 0.659 mm using the commercial software package PUFF. Using the formulae

$$\epsilon_{r,effective} = \frac{2\epsilon_r}{1+\epsilon_r}$$

and

$$\lambda_g = \frac{\lambda_o}{\sqrt{\epsilon_r}}$$

λ_g was found to be 2.268 cms for a stripline. The length of the slot was to be $\frac{\lambda_g}{4}$.

The stripline extended till the centre of the slot which was in line with the centre of the sliding short underneath. Thus, the fields from the stripline coupled with the waveguide of the sliding short. With the length of the short correctly adjusted, there was resonance. The side radiation of the parallel plate guide mode were effectively cancelled out by the reflected waves from the sliding short as evident in 2.2, being out of phase. They then coupled with the slot to be radiated out from there. Thus, with the length of the sliding short properly adjusted, there would be a complete cancellation of the side radiation.

3.3 Fabrication details

The micro-meter type sliding short was a X-band rectangular waveguide of ECIL, Hyderabad make (Model no. X715) with the dimensions of 23mm X 10.5 mm. Its minimum depth (at micrometer setting of zero) was found to be 5.97 mm and maximum of 33.97 mm. The overall setup was as in Fig 3.2.

The length of the radiating slot on the upper ground plane was taken to be $\lambda_g/2$ and the stripline extended till its centre so that there is no coupling between the two. The sliding short was fixed on the lower ground plane with a slot etched there on the substrate of dimensions equal to the waveguide dimensions. The entire structure was held together by four teflon screws of 4mm diameter. Fig 3.3 gives the outline of the rubylith cut for etching of the stripline, slot and the waveguide opening.

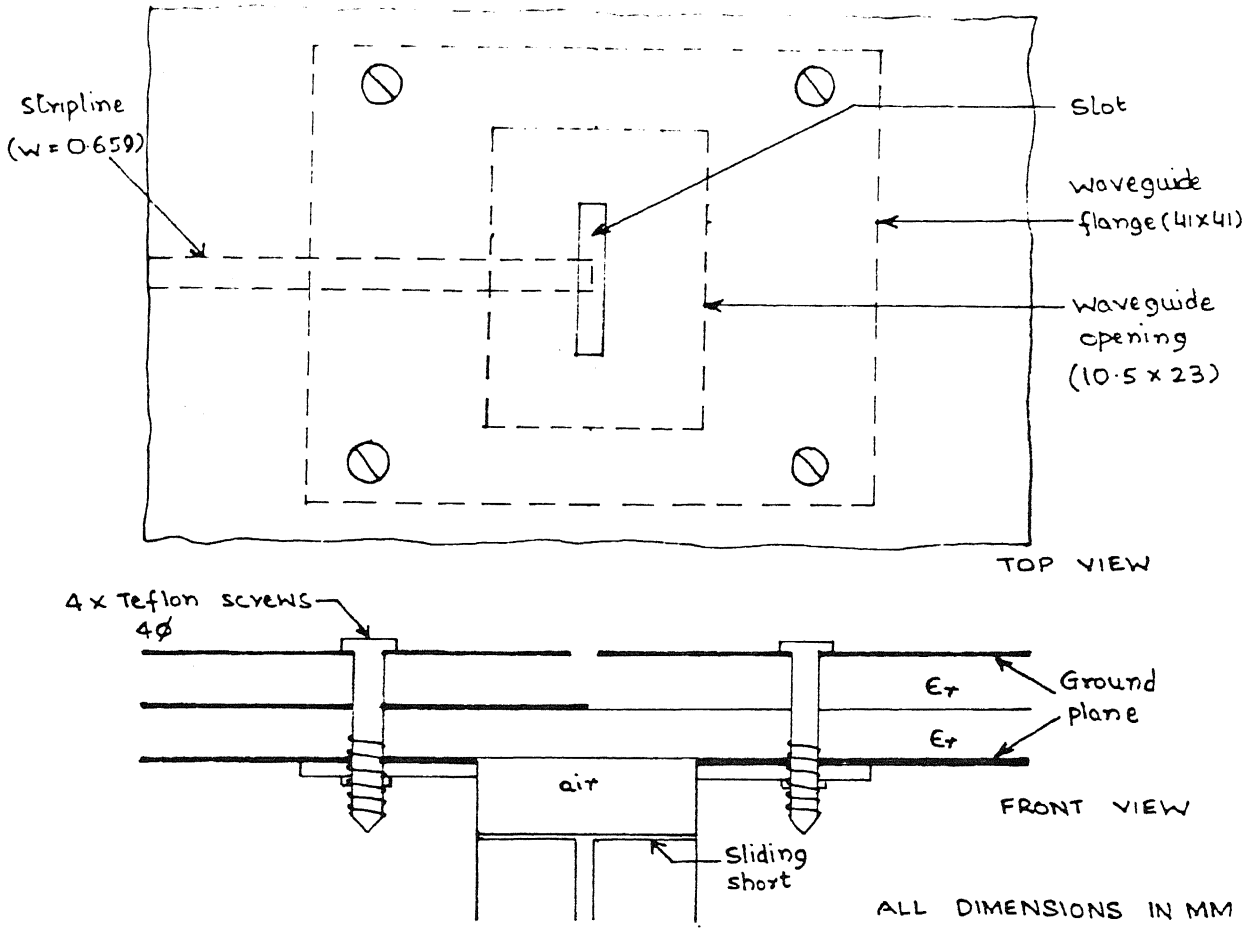

Figure 3.2: Rectangular stripline-fed cavity-backed slot

3.4 Measurement setup and procedure

3.4.1 Introduction

There were mainly two experiments required to be conducted on the antenna structure now fabricated:—

- Measurement and plotting of the S_{11} characteristics Versus the frequency in GHz from 8–12 as the design frequency was 10 GHz. This would give an idea of the matching achieved and the resonant point(s) of the antenna.

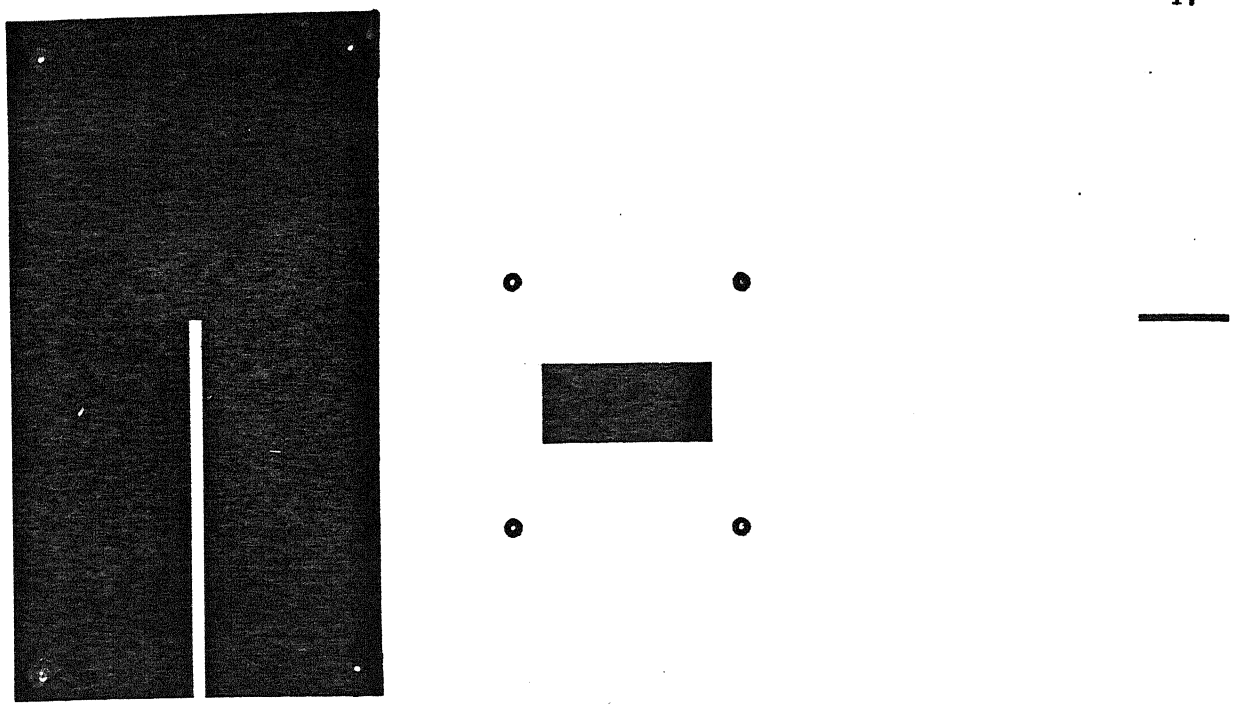

Figure 3.3: Outline of the rubylith cut for the etching

- Radiation plot of the antenna so as to find out the suppression of the parallel plate guide mode achieved vis-a-vis the main lobe.

3.4.2 Measurement of the S_{11} characteristics

The S_{11} measurement was done on the network analyser setup consisting of:—

1. 7.5—12.4 GHz microwave source (Wavetek, model 955)
2. Network analyser set (Hewlett-Packard, model 8410A)
3. S-parameter test set 5—12.4 GHz (Hewlett-Packard, model 87468 Opt 001)
4. Personal computer

A computer program had been made to directly read the S_{11} magnitude and phase information from the Network analyser set for a particular frequency. A data

file so created was utilised for plotting the relevant curves. Starting from a short, the cavity depth was increased and the readings recorded. A total of six readings for cavity depths of 0, 4.72, 5.97, 10.27, 12.92 and 15.2 mm were taken. The descriibed setup is shown in Fig 3.4 .

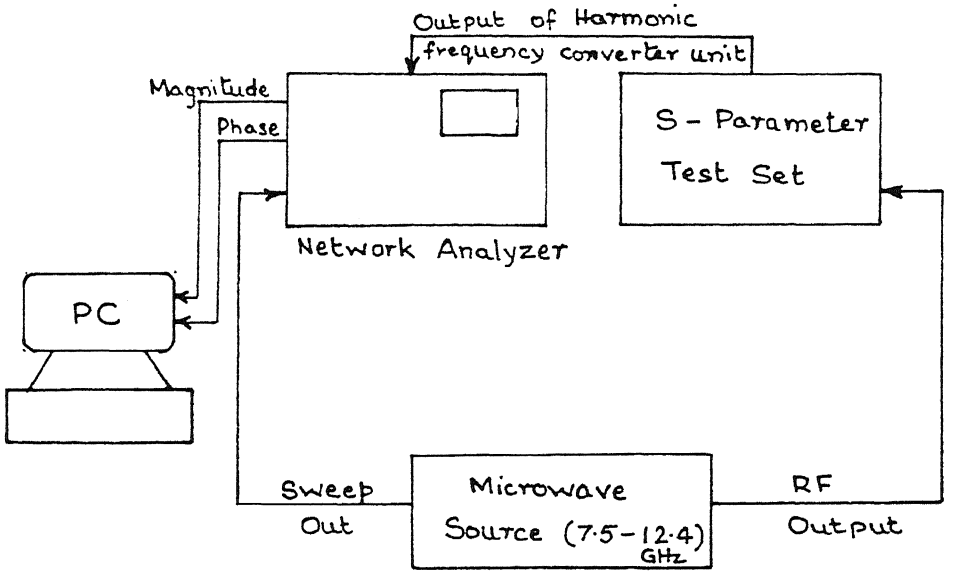

Figure 3.4: Experimental setup for measurement of S_{11} characteristics

When the data so obtained was plotted, it was difficult to judge the amount of parallel plate guide mode suppression as no reference plots were available for these vary cavity depths. Then, it was decided to obtain data for those particular settings with the entire structure shorted around the sides with a thin metallic foil. This represented the ideal case of a total side-radiation suppression. Plots were then taken for various combinations of these curves for easy reference and inference.

3.4.3 Generation of radiation plot

Radiation plots were generated using a spectrum analyser setup consisting of:—

1. Automatic preselector (Hewlett-Packard, model 8445B)

2. Microwave source 7.5—12.4 GHz (Wavetek,model 955)

3. Spectrum analyser (Hewlett-Packard, model 8555A)

The antenna structure was fed with sufficient microwave power from the microwave source. A horn receiver kept 82.6 cms away at exactly the same height as the antenna, picked up the radiations. It was fed to the spectrum analyser set. The antenna was mounted on a stand whiich could be rotated around 360°. Thus, a plot of Received power Versus the Degree of rotation of the antenna was plotted. Like in the S_{11} characteristics similar readings were taken with the side radiations shorted by the metallic foil to give a comparison. The test setup was as shown in Fig 3.5.

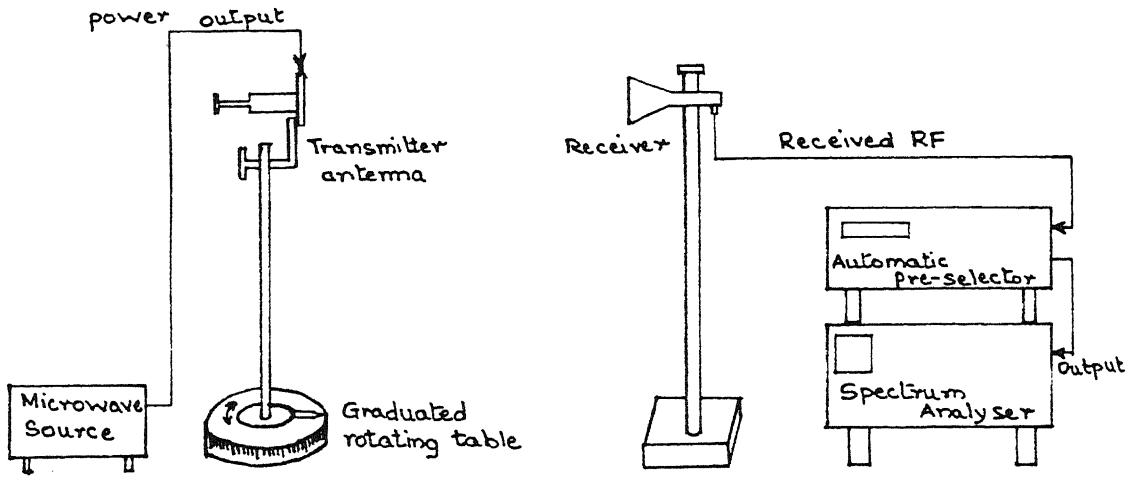

Figure 3.5: Experimental setup for the radiation plot

3.5 Results

All the data got from the two measurements described previously was put in the data files and the curves plotted. Since there were *six* readings each with and without the shorting foils, making up a total of *twelve* curves, it was difficult to plot them all on one or two graphs without sacrificing clarity. Thus, they were split up in convenient lots and plotted as per the details given in Table 3.1 .

Fig No	Cavity Depth(s)(mm)	S_{11} charac	Radiation plot	Without foil	With foil
3.6	0.0, 4.72	√	—	√	√
3.7	5.97, 10.27	√	—	√	√
3.8	12.92, 15.2	√	—	√	√
3.9	0.0, 4.72, 5.97 10.27, 12.92, 15.2	√	—	—	√
3.10	-do-	√	—	√	—
3.11	0.0	—	√	√	√
3.12	5.97	—	√	√	√

Table 3.1 Graphs plotted for Stripline-fed Cavity-backed slot.

One point to note here is that, while the S_{11} characteristic curves have been drawn for all the cavity depths, radiation plots only for cavity depths of 0.0 mm and 5.97 mm have been taken with and without foil. This is so because, when a comparison of the data for powers received at 0° (main lobe radiation) and ±90° (side radiation) for various cavity depths from 0.0 mm to 17.97 mm at intervals of 0.50 mm was done, there was hardly any difference found in the readings. Thus, graphs were plotted only for depths of 0.0mm (no cavity) and 5.97 mm (best suppression).

3.6 Observation

Before the relevant observations are recorded here, it is pertinent to note the following points:—

- The reference line shown (labelled as *short* in all the graphs) is just a short circuit at the antenna input point. It has been placed on the graphs to give an idea of the system noise.

- In all the graphs, the curves taken with a shorting metallic foil around the structure, have been shown in dotted lines, interspersed with asterisks.

On a close study of the graphs plotted, the following observations are made:—

1. Refer Figures 3.6, 3.7 and 3.8. As is expected, all the cavity depths (except 4.72mm) show better S_{11} characteristics with the metallic foils than without. But, for 4.72mm , it is the other way round and the difference at the peaks is about -20 dbs. This is inexplicable specially because the radiation plot at this depth is worse than at 5.97mm depth.

2. Another observation from the same set of graphs emerges that there are multiple resonance points in all the curves. The maximum dip in S_{11} occurs normally around 10.2 GHz (*the design frequency is 10 GHz*). However the dip decreases as the cavity depth increases. Other resonance points are around 8.5 and 9.3 GHz. Resonance at 9.3 GHz does not occur at the two maximum cavity depths.

3. Except for a depth of 10.27mm, the curves for all the depths shift to the right compared to curves with metallic foils for the same depths.

4. From Figure 3.9, which shows all the S_{11} characteristics for cavity depths with-

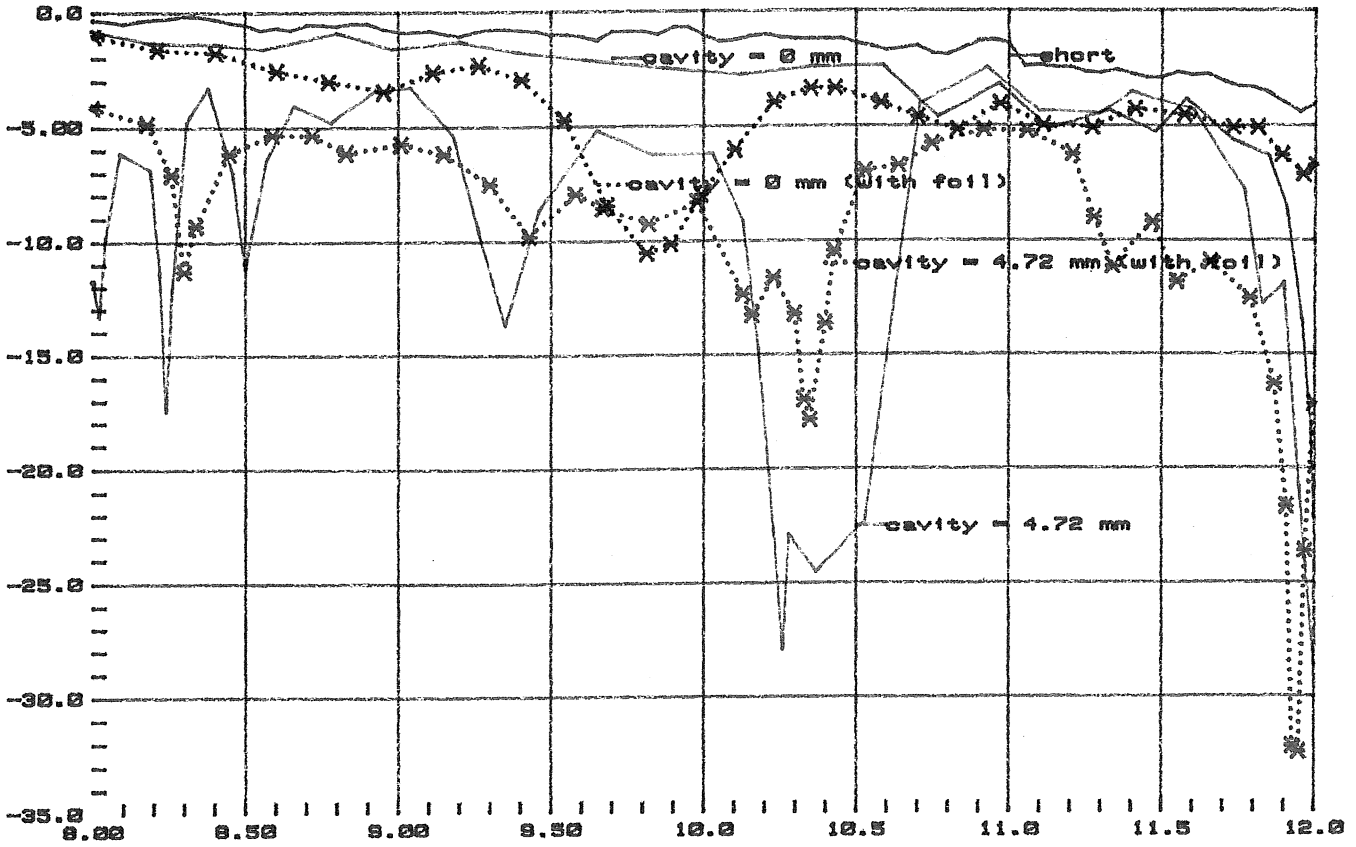

Fig. 3·6

Fig. 3.6. Figure showing variation of Reflection coefficient with Frequency for cavity depths of 0.0mm and 4.72mm, with and without the shorting foils

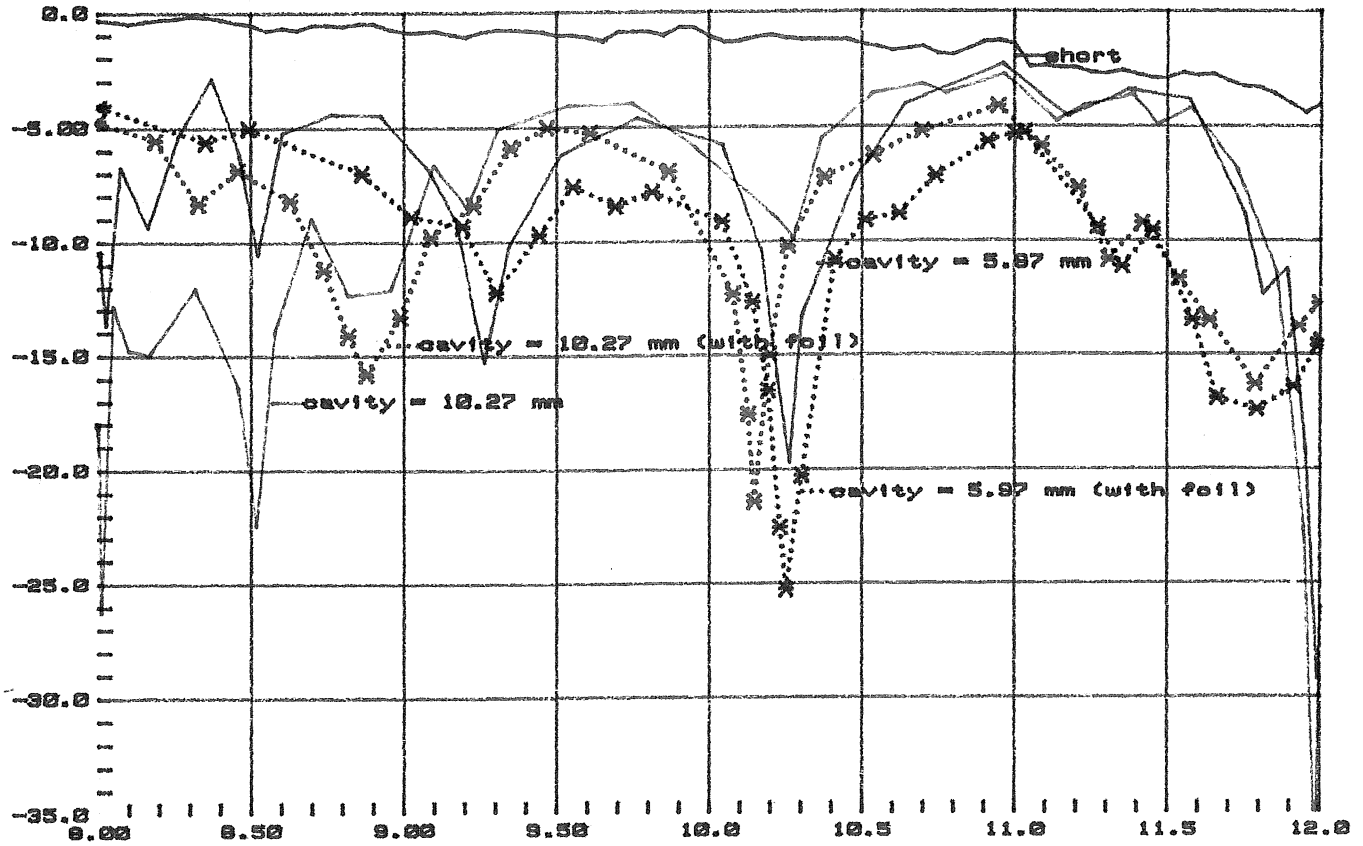

Fig. 3.7

Fig. 3.7. Figure showing variation of Reflection coefficient with Frequency for cavity depths of 5.97mm and 10.27mm, with and without the shorting foils

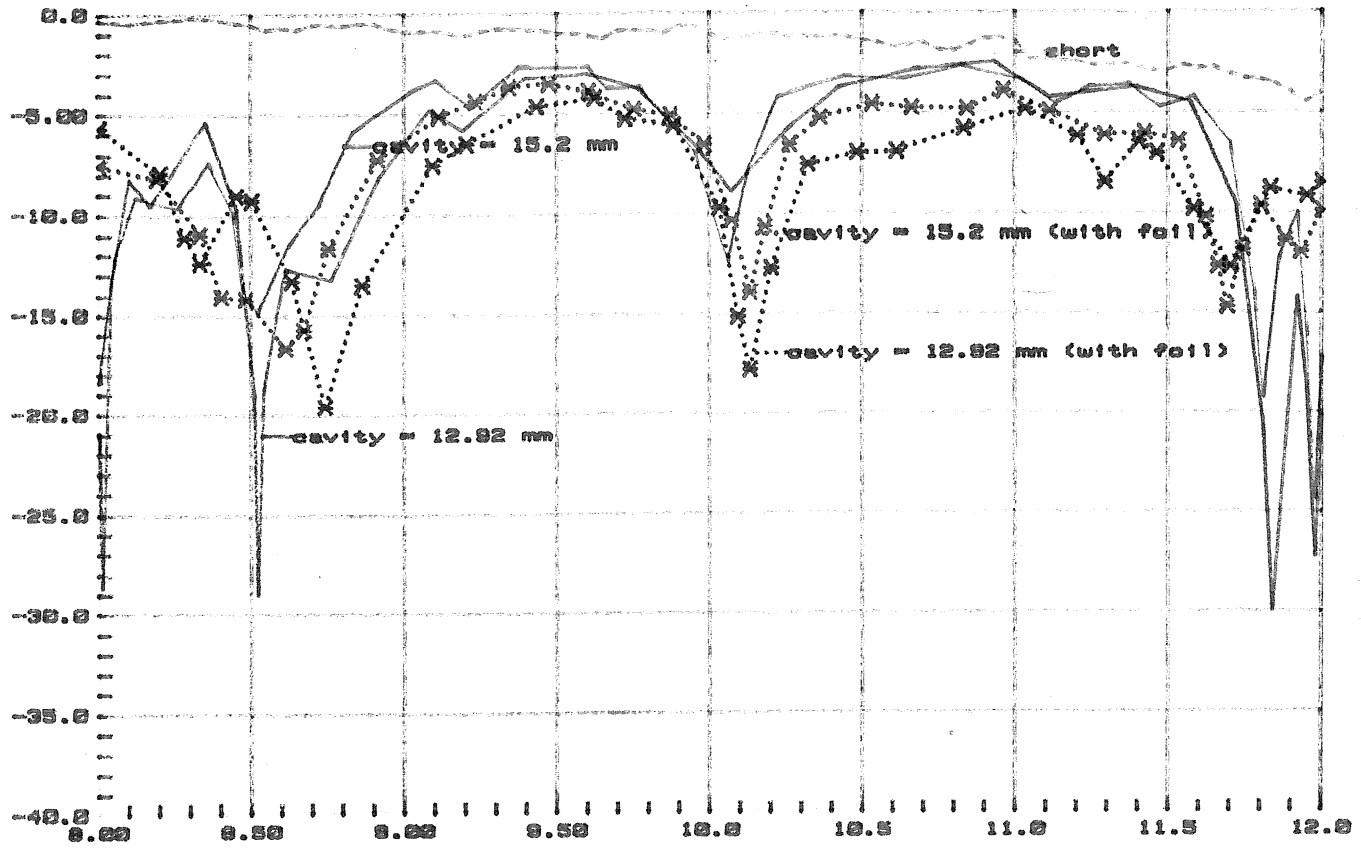

Fig. 3·8

Fig. 3.8. Figure showing variation of Reflection coefficient with Frequency for cavity depths of 12.92mm and 15.2mm, with and without the shorting foils

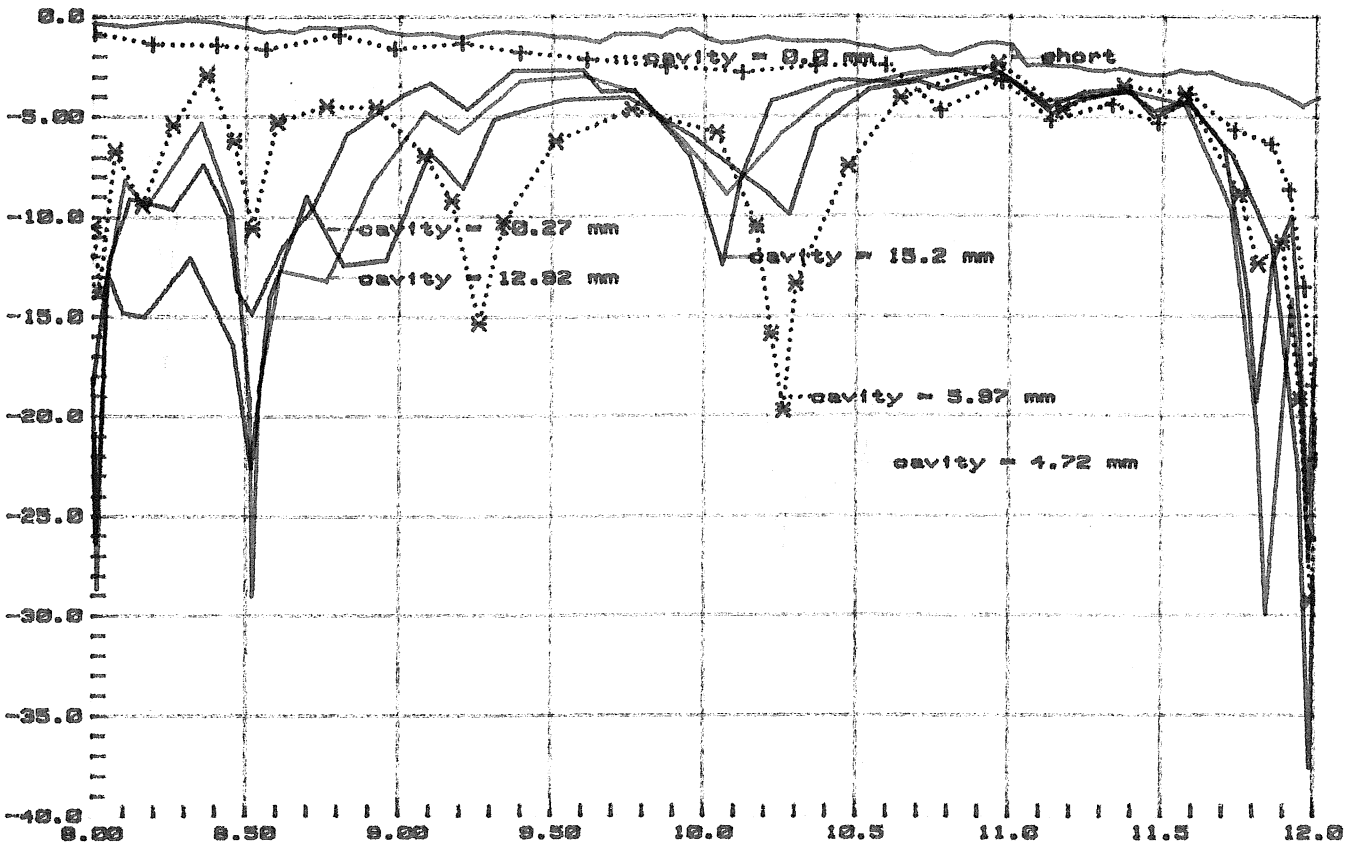

Fig. 3·10

Fig. 3.10. Figure showing variation of Reflection coefficient with Frequency for cavity depths of 0.0mm, 4.72mm, 5.97mm, 10.27mm, 12.92mm and 15.2mm, without shorting foils.

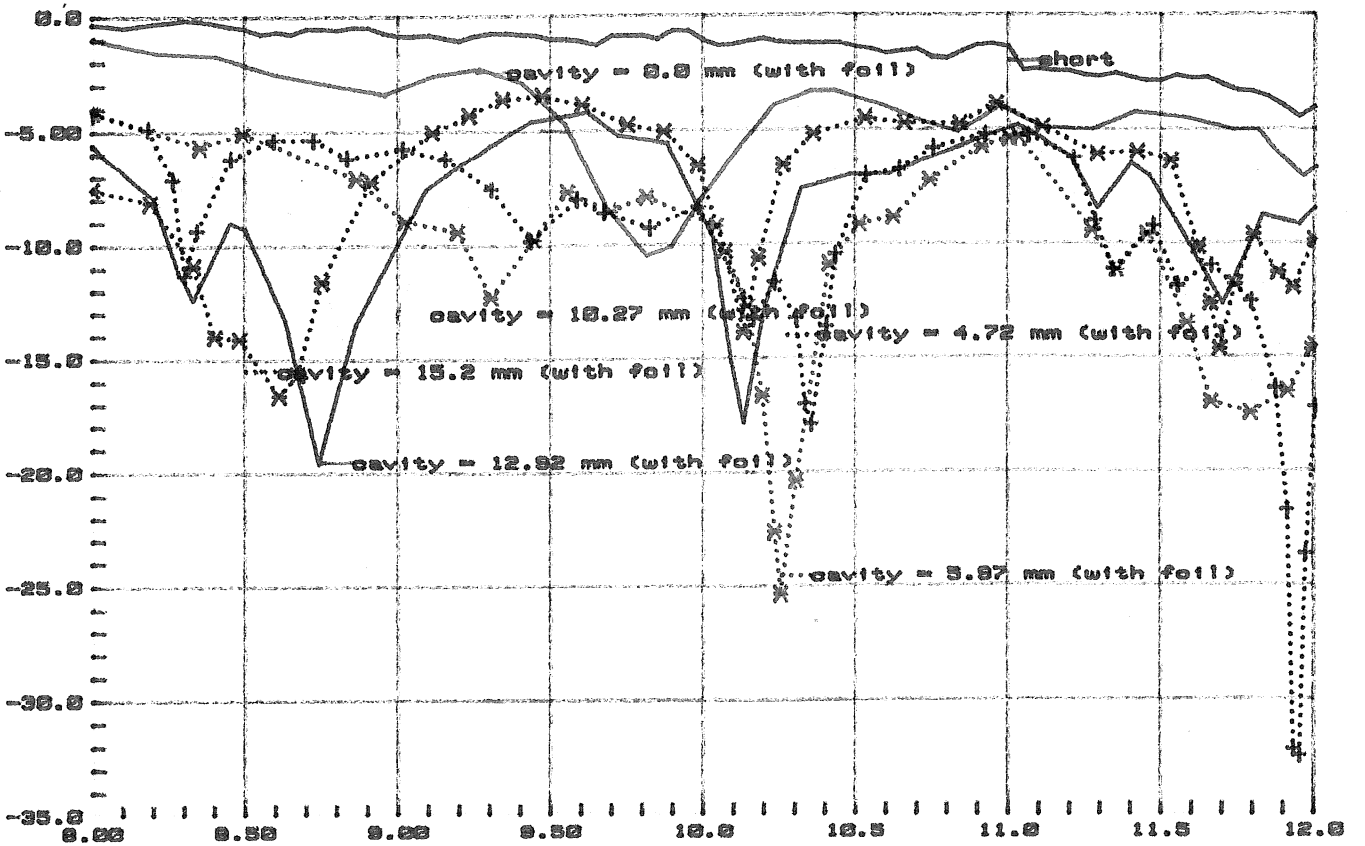

Fig. 3.9

Fig. 3.9. Figure showing variation of Reflection coefficient with Frequency for cavity depths of 0.0mm, 4.72mm, 5.97mm, 10.27mm, 12.92mm and 15.2mm, with shorting foils.

out the foil, it is clear that the resonance points shift to the left (i. e. the resonance frequencies decrease) with increasing cavity depths for resonance around the design frequency. This shift is to the right for resonance around 8.5 to 9.5 GHz. The only exception is the cavity depth of 15.2 GHz.

5. Similar observations are made for the Fig. 3.10 which has curves for structures with metallic foils to suppress side radiations.

6. Fig. 3.11 gives the curves for the radiation plot for a shorted cavity i. e. cavity depth of 0.0mm with and without foil. With foil, when there is no parallel plate guide mode , the curve is almost ideal. There are some irregularities, but they may probably be attributable to the reflections from surrounding objects and the walls as the measurements were made in a closed room. Compared to this, the curve without foil is quite haphazard. The main lobe is shifted by about 45° and there are six prominent side lobes.

7. Fig. 3.12 shows the curves for cavity depth of 5.97mm with and without the metallic foil. With the foil, the main and the side lobes are quite prominent, though not so much as for the shorted cavity with the foil. On comparison of the curves without foil for this case and for the shorted cavity, it is found that, though the main lobe occurs at almost the same point, the number of side lobes is lesser by one with a lesser amplitude in the former case.

3.7 Conclusion

- It is concluded from the S_{11} characteristics that the cavity has not made much of a difference in the resonant points of the antenna structure. Large variations

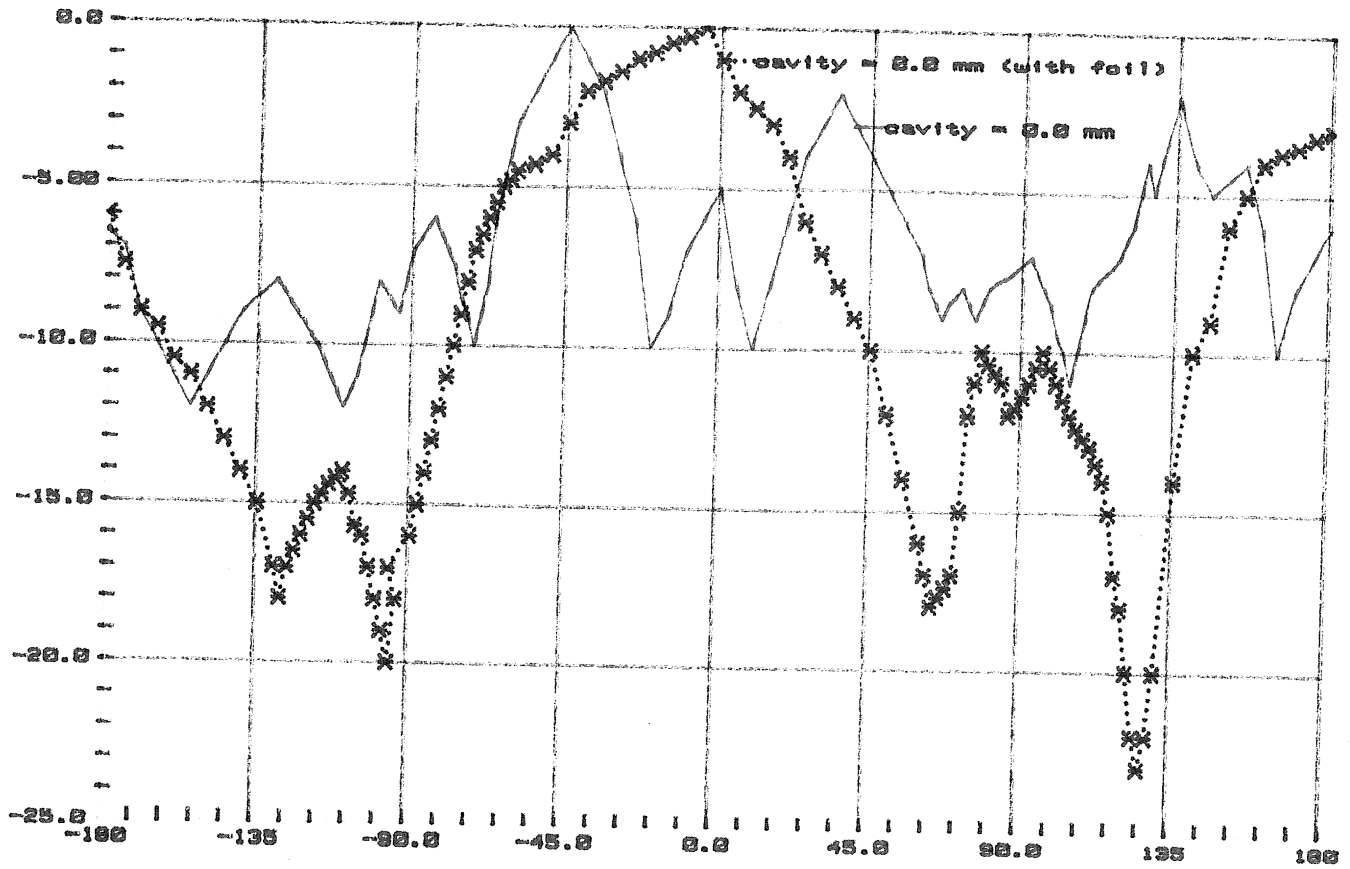

Fig. 3.11

Fig. 3.11. Figure showing variation of Power received with degrees (i.e. the radiation plot) for antennna structure without cavity (cavity = 0.0mm) with and without the shorting foils.

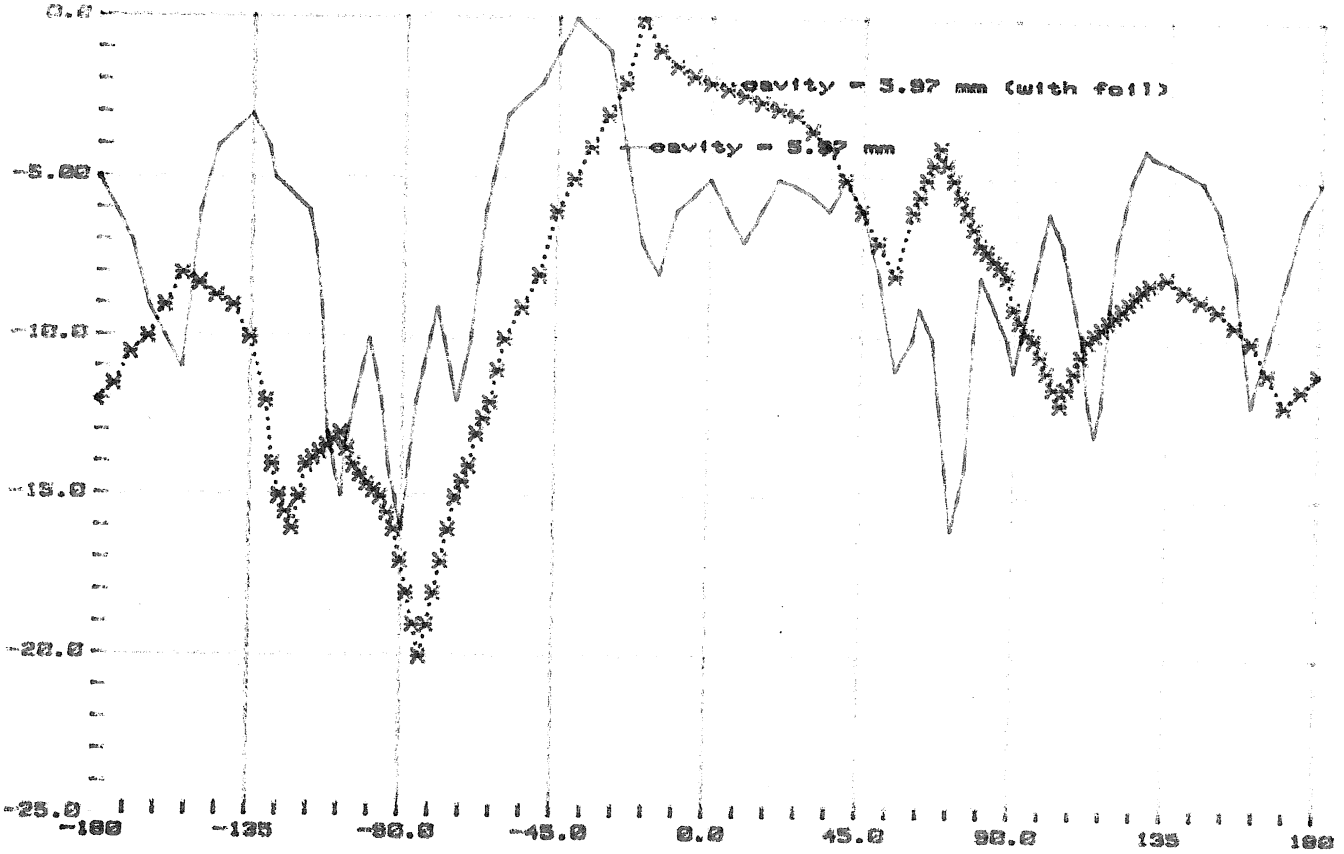

Fig. 3.12

Fig. 3.12. Figure showing variation of Power received with degrees (i.e. the radiation plot) for antennna structure wit cavity depth of 5.97mm with and without the shorting foils.

of cavity just produce minor shifts of resonance points and S_{11} magnitude.

- There is no definite pattern in the shifts and magnitudes of the resonant points for various cavity depths.

- The most important parameter, the radiation plot, which shows up the suppression of the parallel plate guide mode has not been much affected by the presence of cavity. Only the cavity depth of 5.97 mm has been plotted as even large variations of cavity depth did not affect the main and the side radiation appreciably.

- Finally, it is concluded that experimentally, nothing consequential has emerged out of the study conducted for the cavity-backed stripline-fed slot . In fact, the structure is quite complicated to analyse due to various transitions and change of mediums involved. Unless a rigorous analysis is done and a complete knowledge of the fields gained to establish an exact *Quarter wave distance from the centre of stripline to the variable short*, no firm conclusions regarding the feasibility of the structure for this purpose can be drawn.

Chapter 4

Suppression of Parallel Plate Guide Mode Using a Slot Pair

4.1 Introduction

When a slot pair is used in a stripline-fed structure, then both, the individual as well as the mutual impedance come into play. Add to this the parallel plate guide mode effect and the overall recipe does become fairly complicated to analyse and fabricate with precision. While designing and fabricating a slot pair in a stripline structure for the purpose of this study, it was assumed that if individual slot impedances and mutual impedance of the slot pair are taken into account, the point of feeding of the slots can be calculated. However it was found that the parallel plate guide mode has a very profound effect on it and can undermine these calculations to a great extent.

4.2 Design considerations

When transverse or slanted slots are cut in the ground plane of a microstripline, they present a series impedance to the feed line. Y. Yoshimura [6] demonstrated a simple technique of narrowband matching (a few percent of the bandwidth) of the

slot radiator. For available substrate materials and thicknesses, centre–fed transverse slots exhibit high values of normalised to 50Ω radiation impedance; at early stages of study [17] , this was considered a serious obstacle for practical applications of microstrip slot radiators. Typical normalised values of impedance at resonance for the center–fed transverse slot backed by 62 mil thick RT/duroid 5880 ($\epsilon_r = 2.2$) are around 12. In order to overcome this difficulty, Y. Yoshimura shifted the feed point from the centre of the slot and short-circuited the feed microstrip through the dielectric substrate with the slot side which is located further from the feed input. The offset of the feed point leads to perfect impedance matching in a narrow frequency band.

Since in this study, a slot pair was used, the matching of the feed point has to be done taking into account the active impedance of the slot; which in turn takes into account the effects of self as well as the mutual impedance [18].

A centre-fed dipole is one of the very well studied and analysed structures. Established formulae are readily available for calculating the self and mutual impedances of these dipoles. Similarly, there are formulae available to convert these impedances to those of an equivalent slot. Thus, for the calculations for a slot, one can find out the impedances for an equivalent cylinderical centre-fed dipole and convert them to that of a slot using Booker's relationships [18] , [21].

4.2.1 Self impedance of centre-fed cylinderical dipole

When calculating self-impedance of centre-fed cylinderical dipoles by induced EMF method [19], one is able to show that

$$Z = \frac{j60}{sin^2(kl)}[4cos^2(kl) * S(kl) - cos(2kl) * S(2kl) - sin(2kl)[2C(kl) - C(2kl)]] \quad (4.1)$$

$$C(ky) = \ln\frac{2y}{a} - \frac{1}{2}C_{in}(2ky) - \frac{j}{2}Si(2ky) \quad (4.2)$$

$$S(ky) = \frac{1}{2}Si(2ky) - \frac{j}{2}C_{in}(2ky) - ka \quad (4.3)$$

with Si(x) and C_{in} tabulated functions.Here,

Z = self-impedance of centre-fed cylinderical dipole

k = wave number

l = half-length of the dipole

The function Si(x) is called the *sine integral* and is defined by

$$Si(x) = \int_0^x \frac{sinu}{u}du \quad (4.4)$$

whereas the function C_{in} is sometimes called the *modified cosine integral* and is given by

$$C_{in}(x) = \int_0^x \frac{1 - cosu}{u}du \quad (4.5)$$

C. T. Tai [20] has shown that the values of Z computed from above equations are fitted extremely well in the range

$$0 \leq \frac{2l}{\lambda} \leq \frac{\pi}{2}$$

by the expression

$$Z = R(kl) - j[120(\ln(\frac{2l}{a} - 1)cot(kl) - X(kl)] \quad (4.6)$$

with R(kl) and X(kl) smooth, simple functions which he tabulates and graphs. If one represents Tai's functions R(kl) and X(kl) by second degree polynomials with coefficients chosen to fit data computed from the equation 4.1 in the range $1.3 \leq kl \leq 1.7$ and $0.001588 \leq a/\lambda \leq 0.009525$, the final equation that emerges is

$$Z = [122.65 - 204.1(kl) + 110(kl)^2] - j[120(\ln(\frac{2l}{a} - 1)cot(kl) - 162.5 + 140kl - 40(kl)^2] \quad (4.7)$$

For the specified range of dipole lengths and diameters, this equation's real part does not deviate from the induced EMF expression in equation 4.1 by more than 0.42 Ω. The imaginary part of equation 4.7 stays within 2.33 Ω of equation 4.1 with an rms error of 0.20 Ω. Equation 4.7 which can be used with a pocket calculator, is a much simpler equation to use than 4.1.

4.2.2 Mutual admittance of centre-fed cylinderical dipoles

Refer Fig 4.1 where two parallel cylinderical dipoles have been placed a distance y apart, their centres displaced vertically by z and the length of the two dipoles be $2l_1$ and $2l_2$ respectively. Both have the same x coordinates. It is clear that a point on

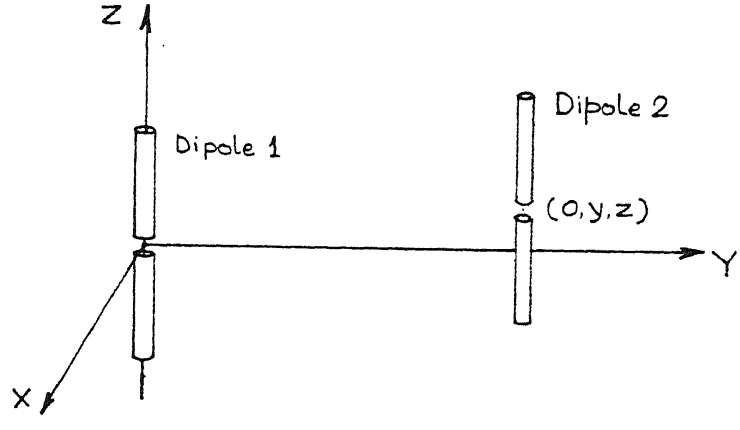

Figure 4.1: Two parallel cylinderical dipoles

the axis of dipole 2 has the co-ordinates $(0, y, z + \xi_2)$ with the central point of dipole 2 at the arbitrary position $(0, y, z)$ in the YZ-plane. It can be written that [18]

$$Z_{12} = \frac{j30}{sin(kl_1) * sin(kl_2)} * \int_{-l_2}^{l_2} [\frac{\exp^{-jkr_1}}{r_1} + \frac{\exp^{-jkr_2}}{r_2} - (2cos(kl_1)\frac{\exp^{-jkr}}{r})] * sin[k(l_2 - \mid \xi_2 \mid]d\xi_2 \quad (4.8)$$

with

$$r = [y^2 + (z + \xi_2)^2]_{1/2}$$

$$r_1 = [y_2 + (z + \xi_2 - l_1]^{1/2}$$

$$r_2 = [y - 2 + (z + \xi_2 + l_1]^{1/2}$$

where

Z_{12} = mutual impedance of the two cylinderical dipoles.

4.2.3 Active impedance of centre-fed rectangular slots

If t be the thickness of the stripline ground plane, w be the width of the strip dipole and a be the radius of the equivalent cylinderical dipole, we have [18]

$$t = w/4 \quad (4.9)$$

$$a = \frac{w + t}{4} \quad (4.10)$$

There is enough literature available along with the design formulae for calculating self and mutual impedance of a cylinderical dipole pair. Using them, Booker's relationship [21] can be applied to convert these impedances to the corresponding self and mutual impedances of a rectangular slot. Its active impedance can then be found out. The Booker's relationship is

$$\frac{Z}{Y} = \frac{\eta^2}{4} \quad (4.11)$$

where η = characteristic impedance of free space = 377 Ω

Z = Impedance of strip dipole

Y = Admittance of rectangular slot

Once the self impedance and mutual admittance of the slot is calculated, it is easy to calculate the active impedance of the centre-fed slot.

If we consider a set of N arbitrarily placed slots in a common large ground plane, this array can be viewed as an N-port linear bilateral system. If (V_m^s, I_m^s) are the applied voltage and the input current at the m^{th} slot, then one can write [18]

$$I_m^s = \sum_{n=1}^{N} V_n^s Y_{mn}^s$$

with Y_{mm}^s the self admittance of the m^{th} slot and Y_{mn}^s the mutual admittance between the m^{th} and the n^{th} slots. Thus, in this study, it becomes

$$\begin{bmatrix} I_1 \\ I_2 \end{bmatrix} = \begin{bmatrix} Y_{11} & Y_{12} \\ Y_{21} & Y_{22} \end{bmatrix} \begin{bmatrix} V_1 \\ V_2 \end{bmatrix}$$

As excitation of both the slots is to be the same, $I_1 = I_2$ and $V_1 = V_2$. Also, as both the slots are to be of equal dimensions, $Y_{11} = Y_{22}$ and $Y_{12} = Y_{21}$. Then,

$$\begin{bmatrix} I \\ I \end{bmatrix} = \begin{bmatrix} Y_{11} & Y_{12} \\ Y_{12} & Y_{11} \end{bmatrix} \begin{bmatrix} V \\ V \end{bmatrix}$$

$\Rightarrow \frac{I}{V} = Y_{11} + Y_{12} = Y_{active} = Y_a$

After calculation of Y_a, the amount of offset can be calculated by the formula,

$$Z_a sin^2\theta = Z_{line} \tag{4.12}$$

where

$Z_a = Z_{active}$

Z_{line} = Z of feed line

θ = Distance in degrees from the edge of the slot (total length = 180°)

4.3 Fabrication details

The substrate used is RT/duroid of $\epsilon_r = 2.2$ and thickness, t = 0.794mm.

For calculation of Z and Z_{12} of cylinderical dipole, computer programs were made. Computer programs helped in optimizing the various dimensions of the slots and their spacing so that the overall structure resonated (i. e. imaginary part of equations 4.7 and 4.8 kept very low, if not exactly zero).

It was found that a slot width of 1.4mm, length of 13.6mm and spacing of 8.9mm between the slots led to

$$Z_{11} = 54.762 - j0.2516$$

and

$$Z_{12} = -40.04 - j1.09$$

With the imaginary parts of both the impedances very low, these dimensions were adopted.

On calculating $Y_{11_{slot}}$ and $Y_{12_{slot}}$ and then Y_{active}, it was found that

$$Z_{active} = 2410.0848\Omega$$

This is for double sided radiation. For single sided radiation with a ground plane on one side, this value gets doubled. Calculating the offset from equation 4.12, the offset was found to be 7.3° which corresponds to 0.55mm for a stripline of 78Ω impedance.

An impedance of 78Ω was used for the line because a lower impedance would have resulted in the feed point going partly out of the edge of the slot, thus weakening the coupling between the two. A higher impedance would have made the lines too thin to be etched comfortably.

The width of the various lines in the overall design in Fig 4.2 was calculated using the PUFF software package. The tuning stub of $\lambda_g/4$ length was reduced by a

distance Δl to take into account the fringing field effects at the stub end. The length Δl is given by [22]

$$\Delta l = c\frac{c + 2w}{4c + 2w}$$

where

$c = \frac{b}{\pi} \ln 2$

in which

w = width of the line

b = thickness of the line

Here, it was found to be 0.2mm. The overall design that emerged was as in Fig 4.2. This design was made with an offset of 0.5mm. However, when it was put to test, it was found to be barely radiating. It was then discovered that, in spite of correctly calculating the impedances, dimensions and the offset, there was hardly any coupling between the transmission line and the slots. Also, the resonance was occurring at a point far away from the design frequency. When the offset was increased to 0.9mm, it was found that the coupling improved and the antenna radiated better. The structure was, then, refabricated with the facility of moving the top substrate (with the slot etched on it) with respect to the bottom substrate containing the feed lines. So, effectively the offset was varied. Also, the length of the slot was marginally increased by 0.1mm.

4.4 Measurement setup and procedure

The measurements to be carried out on this antenna were to be the same as for the cavity-backed stripline-fed slot as the aim remained te same. This would have led to

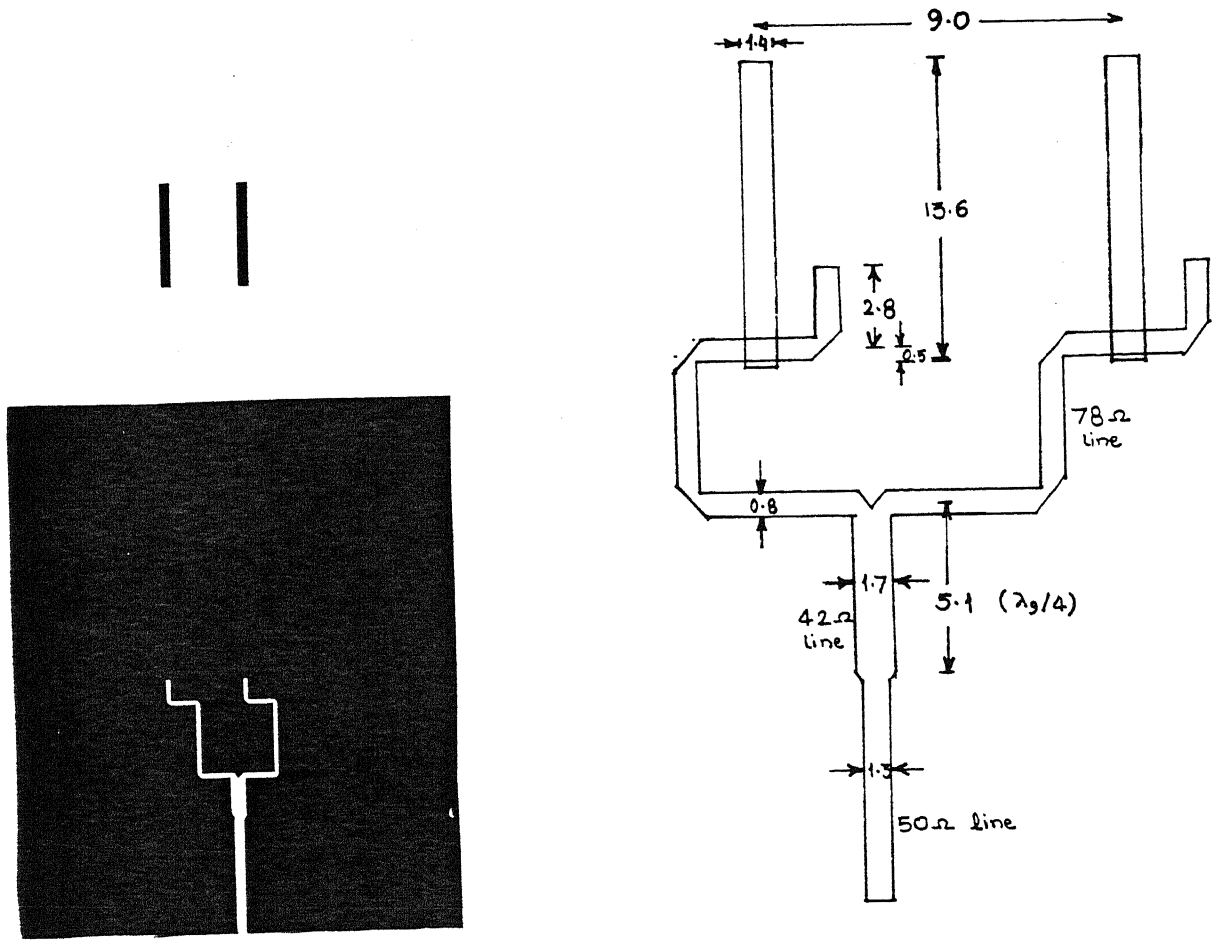

Figure 4.2: Design of the stripline-fed slot pair

using the same two sets of experimental setups — one for the measurement of S_{11} characteristics , and another for the radiation plot.

By the time these tests were to be carried out, another setup was made available for this thesis work which greatly facilitated these measurements. Here, the measurements were totally automated using a PC and one setup sufficed for taking the S_{11} as well as the radiation plot readings. The setup consisted of the following equipments:—

1. Power meter (Hewlett-Packard, model 437B)

2. Synthesised CW source 2–20 GHz (Lucas Weinschel, model 4381)

3. Power sensor (Hewlett-Packard, model 8481A)

4. Dual directional coupler (Hewlett-Packard, model 11692 D)

5. Personal computer

The setup was as shown in Fig 4.3. For calculating the S_{11} characteristics, the

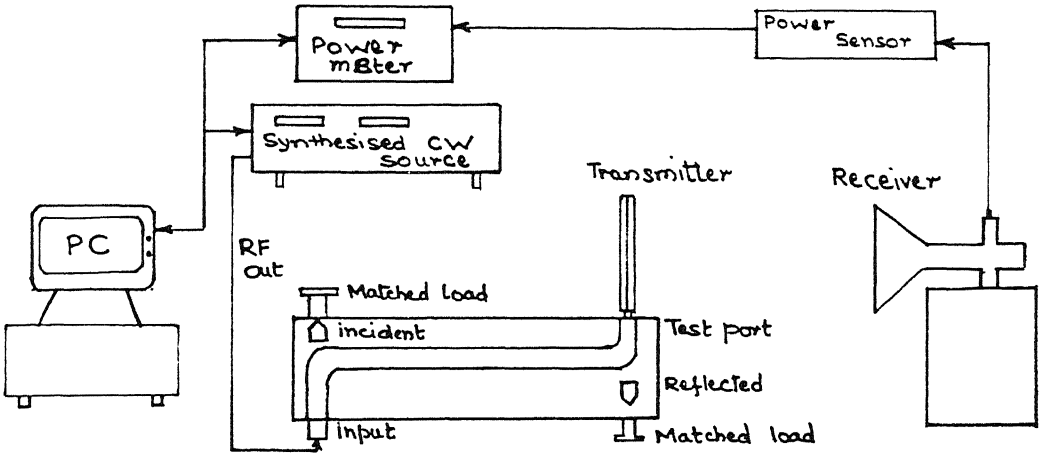

Figure 4.3: Experimental setup for the stripline-fed slot pair

horn was disconnected and the port was terminated by a matched load. The PC directly read the frequency from the CW source and the power received by the Power sensor.Thus, data files were directly made which could be plotted using any grapher program.

4.5 Results

The setup described in Fig 4.3 directly gave the S_{11} characteristics and the radiation power recieved Vs. the frequency. Thus, S_{11} characteistics, and the main and the side lobe patterns for varying frequency from 8—12 GHz could be plotted.

As has already been explained earlier, the final structure used had the facility of varying the slot offset. Later, another structure too was fabricated, the only difference being in the length of the slots. Here, the length of the slots was greater by 1mm.

From the readings taken, a total of twelve graphs were plotted as per the details in Table 4.1.

Fig no	Offset (mm)	Length of slot (mm)	S_{11} characteristics	Main lobe	Side radiation
4.4	0.5	13.6	√	√	√
4.5	0.9	14.1	√	√	√
4.6	1.0	14.2	√	√	√
4.7	2.0	14.2	√	√	√
4.8	3.0	14.2	√	√	√
4.9	4.0	14.2	√	√	√
4.10	4.5	14.2	√	√	√
4.11	4.5	15.2	√	√	√
4.12	2.0	15.2	√	√	√
4.13	0.5,1.0,2.0 4.0,4.5,2.0	13.6,14.2,14.2 14.2,15.2,15.2	√	—	—
4.14	0.5,2.0,4.0,2.0	13.6,14.2,14.2,15.2	—	√	—
4.15	0.5,2.0,4.0,2.0	13.6,14.2,14.2,15.2	—	—	√

Table 4.1 Details of graphs plotted for Stripline-fed slot pair.

4.6 Observations

On a close study of the plotted graphs, the following observations have been made:—

1. S_{11} *charateristics.* Figures 4.4 till 4.12 depict the S_{11} characteristics of various settings of the experiment. Fig. 4.13 depicts the same for six of the most prominent curves for a direct comparison. The following observations on the S_{11} characteristic curves are forwarded:—

   - A study of Figs. 4.4 to 4.12 and 4.13 show that the S_{11} characteristics improve with increasing offsets. In Fig. 4.4, at the design offset of 0.5mm and length of 13.6mm, S_{11} characteristics are very poor.
   - It can be seen from Figs. 4.5 to 4.12, that as the slot length is increased by 0.6mm from 13.6mm to 14.2mm, the characteristics improve. But, there are multiple resonance points in the characteristics.
   - With increase in slot length, the expected shift in the resonance points is negligible.
   - The offset could not be increased beyond 4.5mm due to practical limitations of the design.
   - The best resonance occurs at 10.7 GHz though there is resonance at around 9.9 GHz too. The design frequency is 10 GHz.

2. *Main lobe characteristics.* Figs. 4.4—4.12 depict the main lobe characteristics of the various settings of the experiment. Fig. 4.14 has the chosen four out of the above.

   - The main lobe level i. e. the power received by the receiver for the broad side is low with a low offset, in line with the S_{11} characteristics. As the offset is increased, the coupling between the slots and the feedline is increased. Therefore, the power of the main lobe lobe is increased. This is

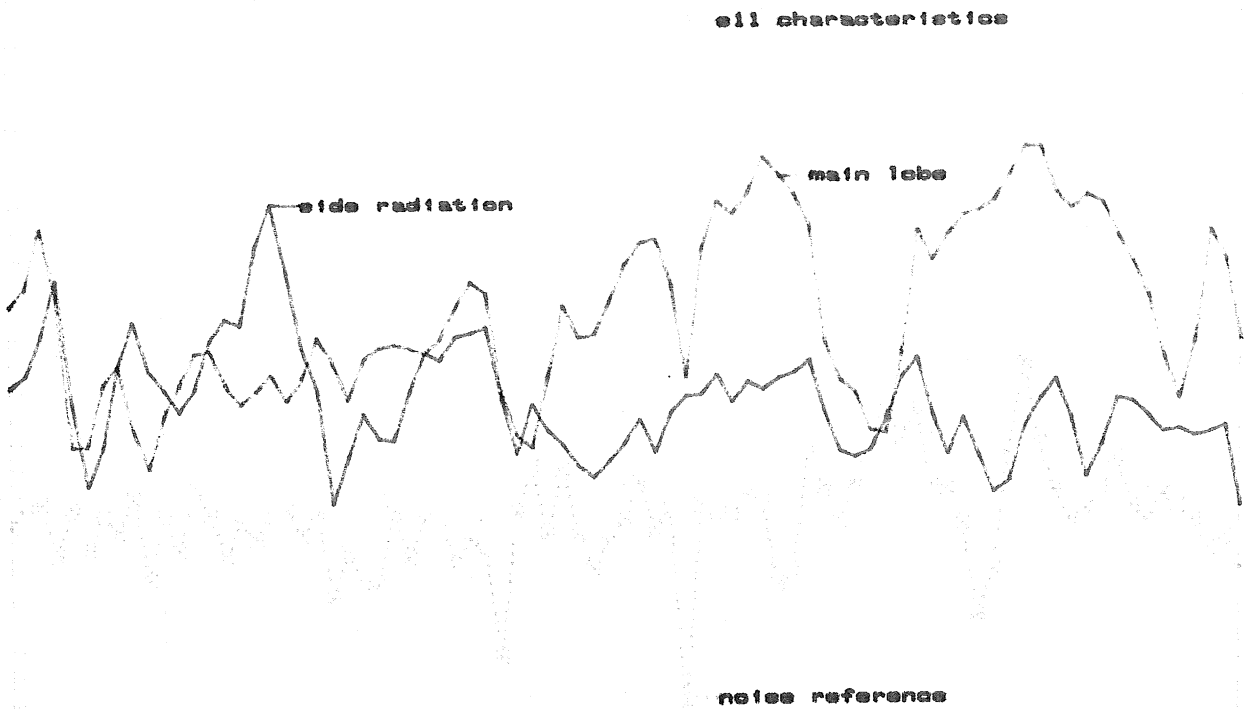

Fig. 4.4. Figure showing the variation of reflection coefficient, main lobe radiation and the side lobe radiation with frequency for an offset of 0.5mm and length of slots of 13.6mm.

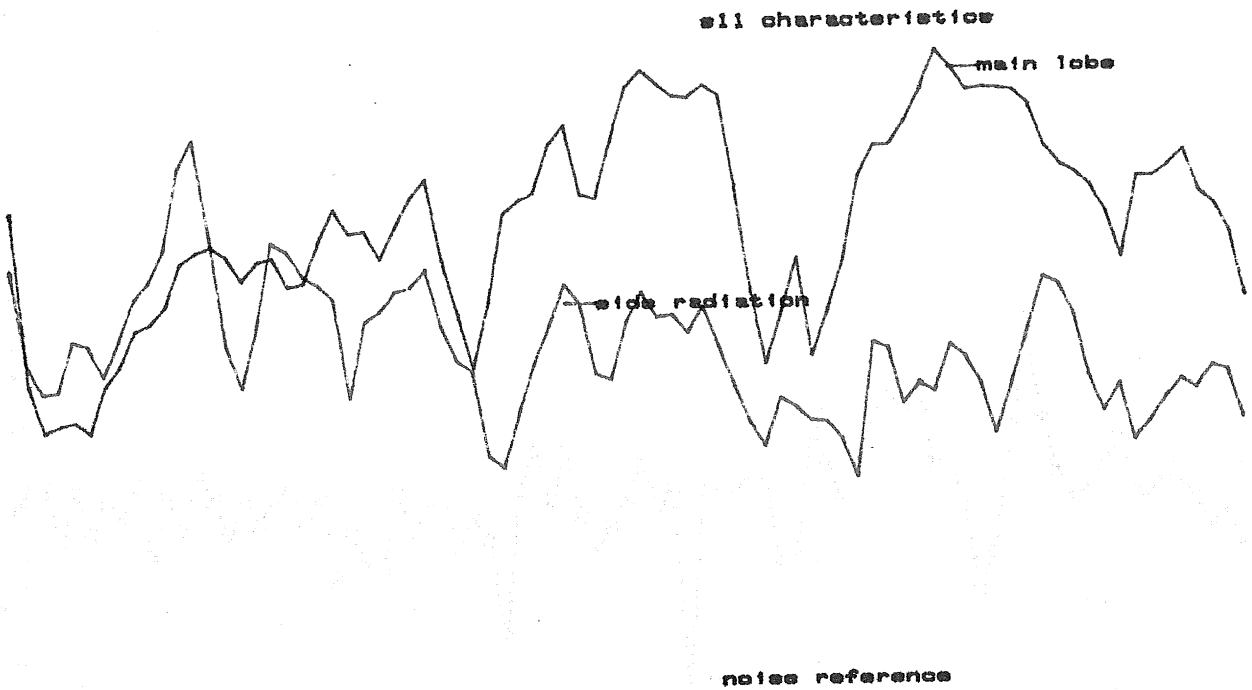

LENGTH OF SLOT = 14.1mm ; OFFSET = 0.9mm

Fig. 4.5. Figure showing the variation of reflection coefficient, main lobe radiation and the side lobe radiation with frequency for an offset of 0.9mm and length of slots of 14.1mm.

Graphstar

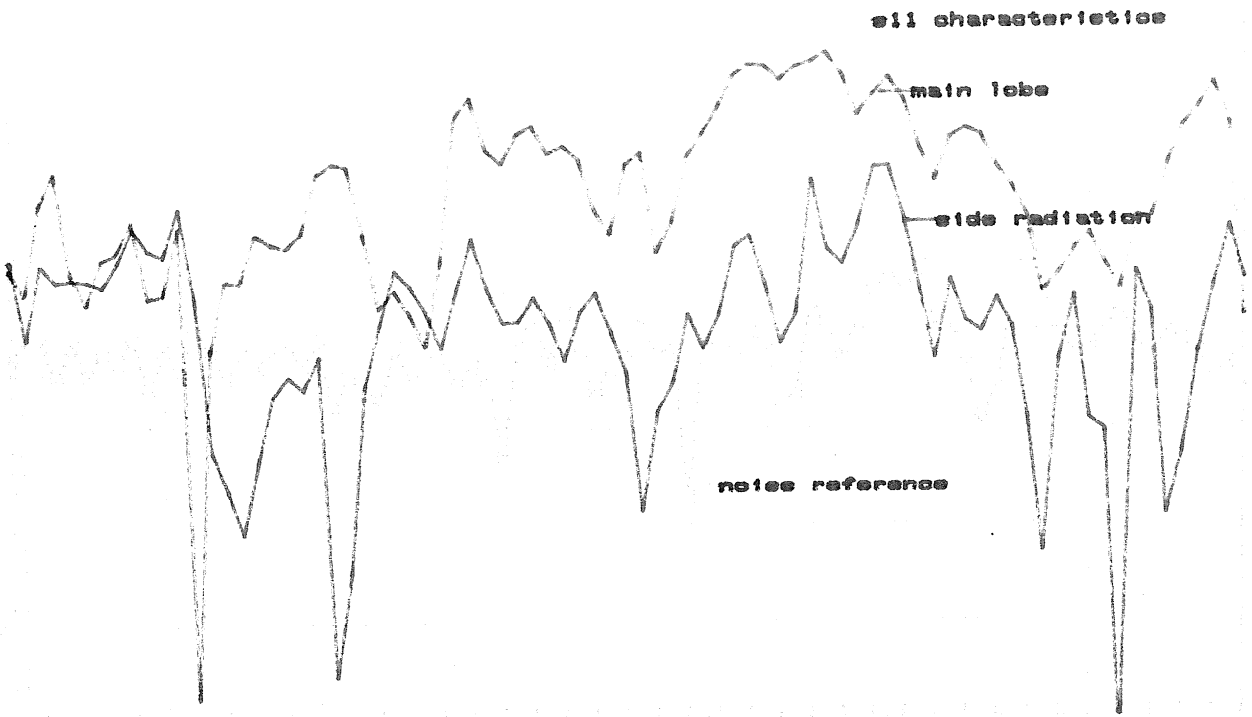

4.6

LENGTH OF SLOT = 14.2mm ; OFFSET = 1.0mm

Fig. 4.6. Figure showing the variation of reflection coefficient, main lobe radiation and the side lobe radiation with frequency for an offset of 1.0mm and length of slots of 14.2mm.

Graphstar

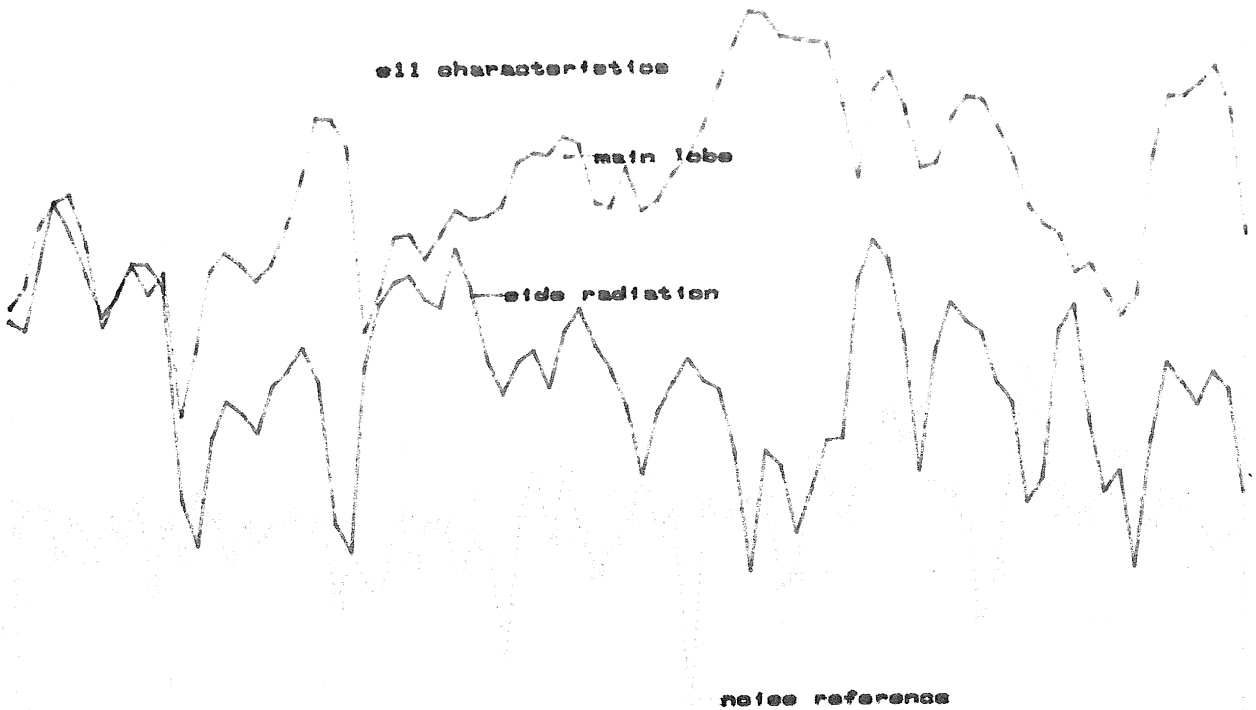

4.7

LENGTH OF SLOT = 14.2mm ; OFFSET = 2.0mm

Fig. 4.7. Figure showing the variation of reflection coefficient, main lobe radiation and the side lobe radiation with frequency for an offset of 2.0mm and length of slots of 14.2mm.

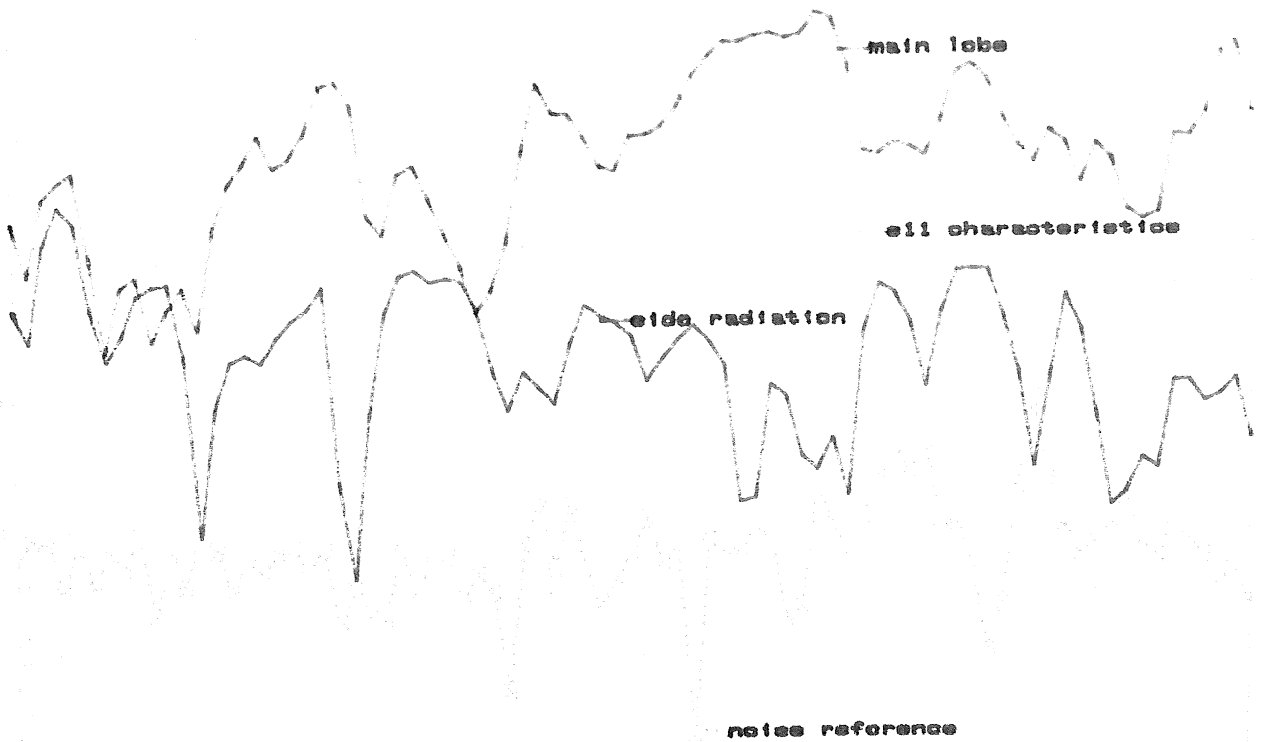

Fig. 4.8. Figure showing the variation of reflection coefficient, main lobe radiation and the side lobe radiation with frequency for an offset of 3.0mm and length of slots of 14.2mm.

uphstar

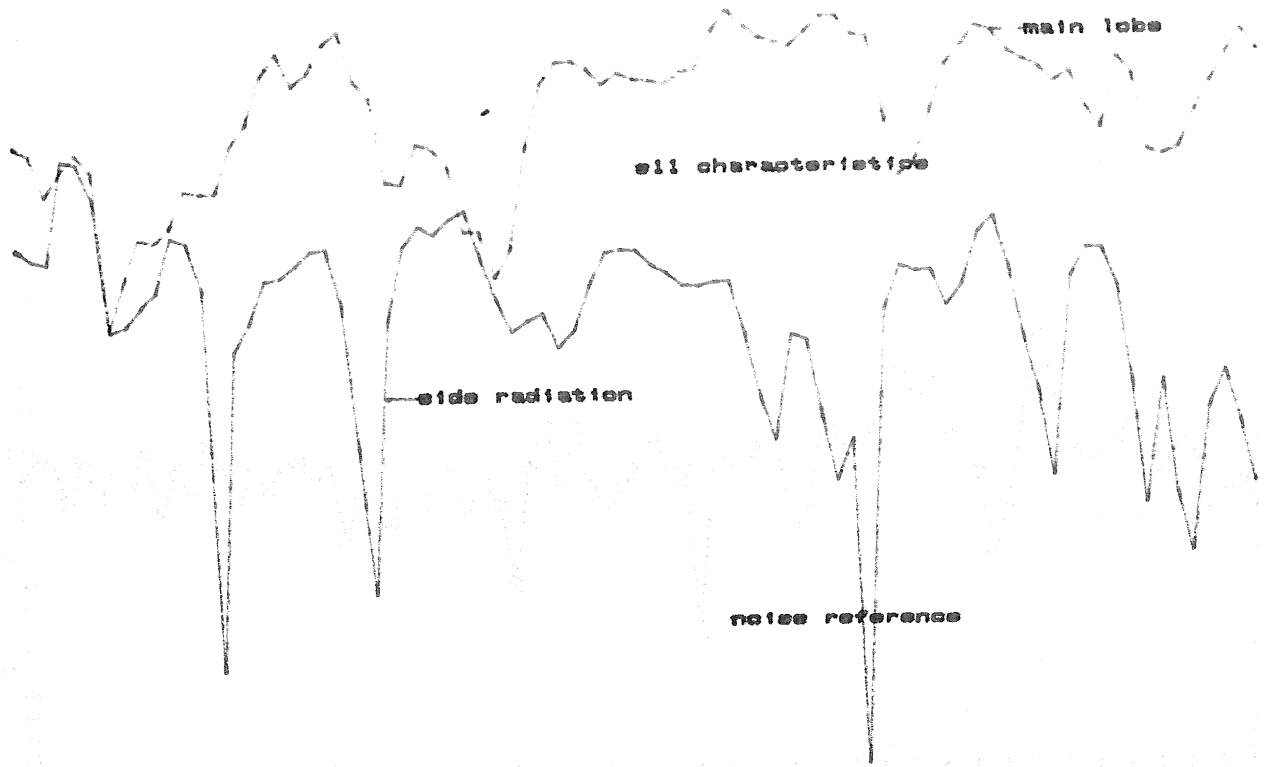

Fig. 4.9. Figure showing the variation of reflection coefficient, main lobe radiation and the side lobe radiation with frequency for an offset of 4.0mm and length of slots of 14.2mm.

Graphstar

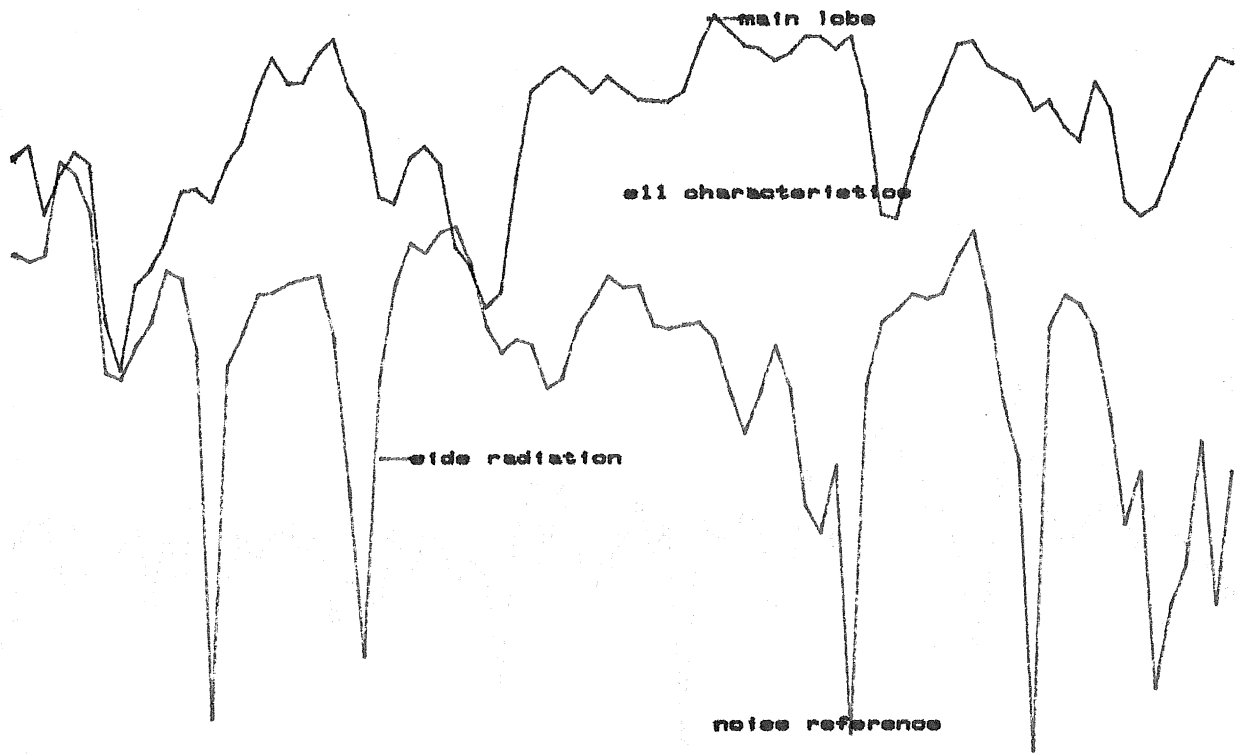

4.10

LENGTH OF SLOT = 14.2mm ; OFFSET = 4.5mm

Fig. 4.10. Figure showing the variation of reflection coefficient, main lobe radiation and the side lobe radiation with frequency for an offset of 4.5mm and length of slots of 14.2mm.

. star

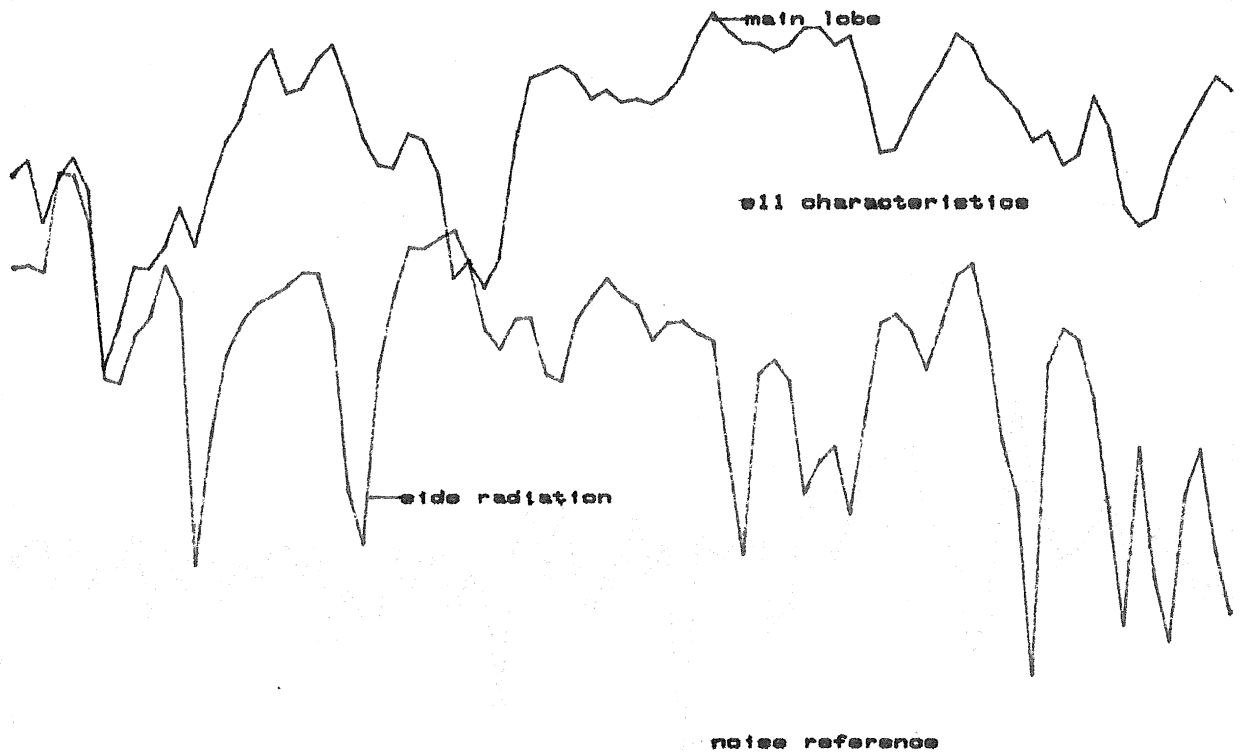

4.11

LENGTH OF SLOT = 15.2mm ; OFFSET = 4.5mm

Fig. 4.11. Figure showing the variation of reflection coefficient, main lobe radiation and the side lobe radiation with frequency for an offset of 4.5mm and length of slots of 14.2mm.

Graphstar

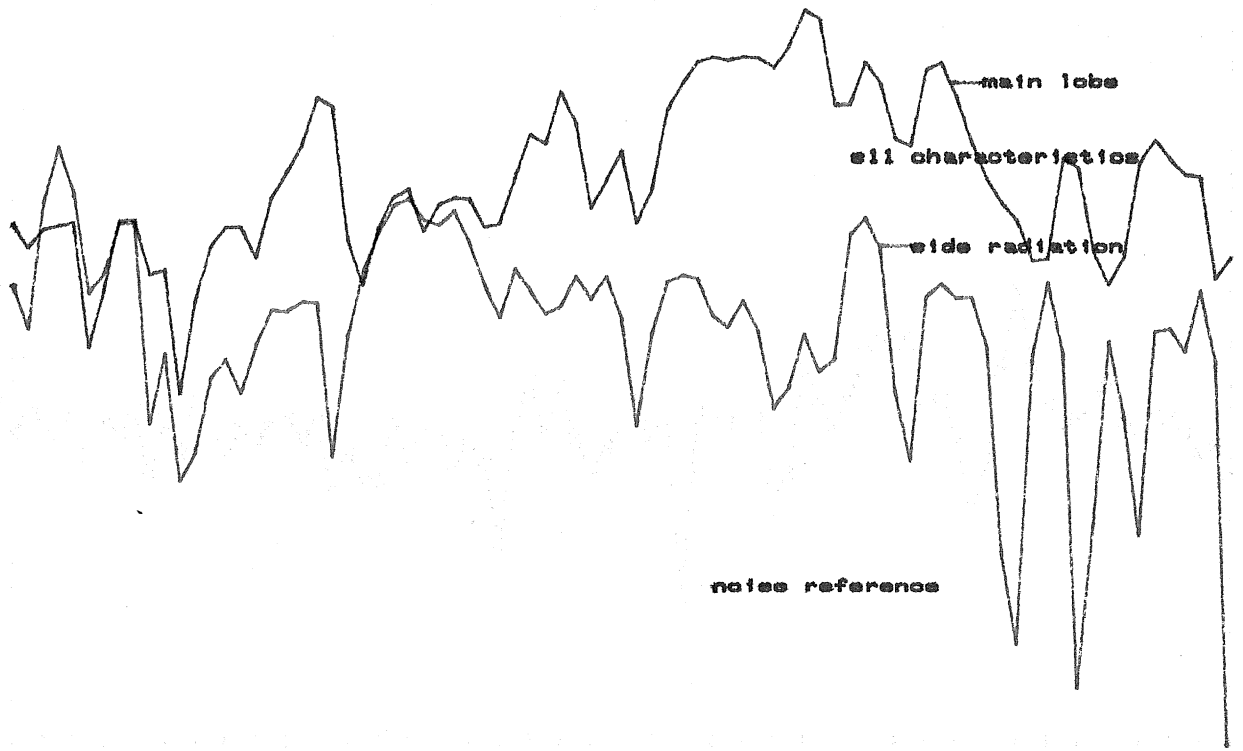

4.12

LENGTH OF SLOT = 15.2mm ; OFFSET = 2.0mm

Fig. 4.12. Figure showing the variation of reflection coefficient, main lobe radiation and the side lobe radiation with frequency for an offset of 2.0mm and length of slots of 14.2mm.

Graphstar

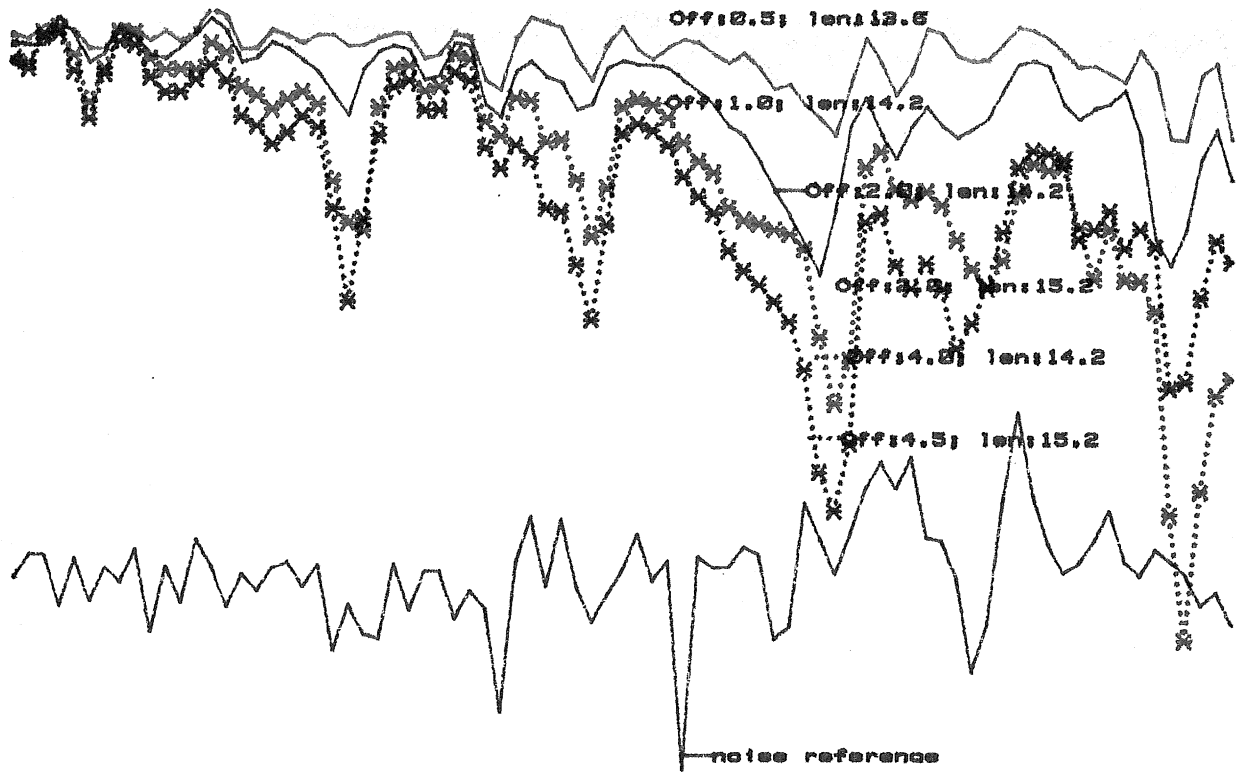

4.13

LEGEND ---> Off: Offset , len: length of slots

Fig. 4.13. Figure showing the comparisons of the variation of reflection coefficient with frequency with the offset and the length of slots settings of Figs. 4.4, 4.6, 4.7, 4.9, 4.11 & 4.12. hetar

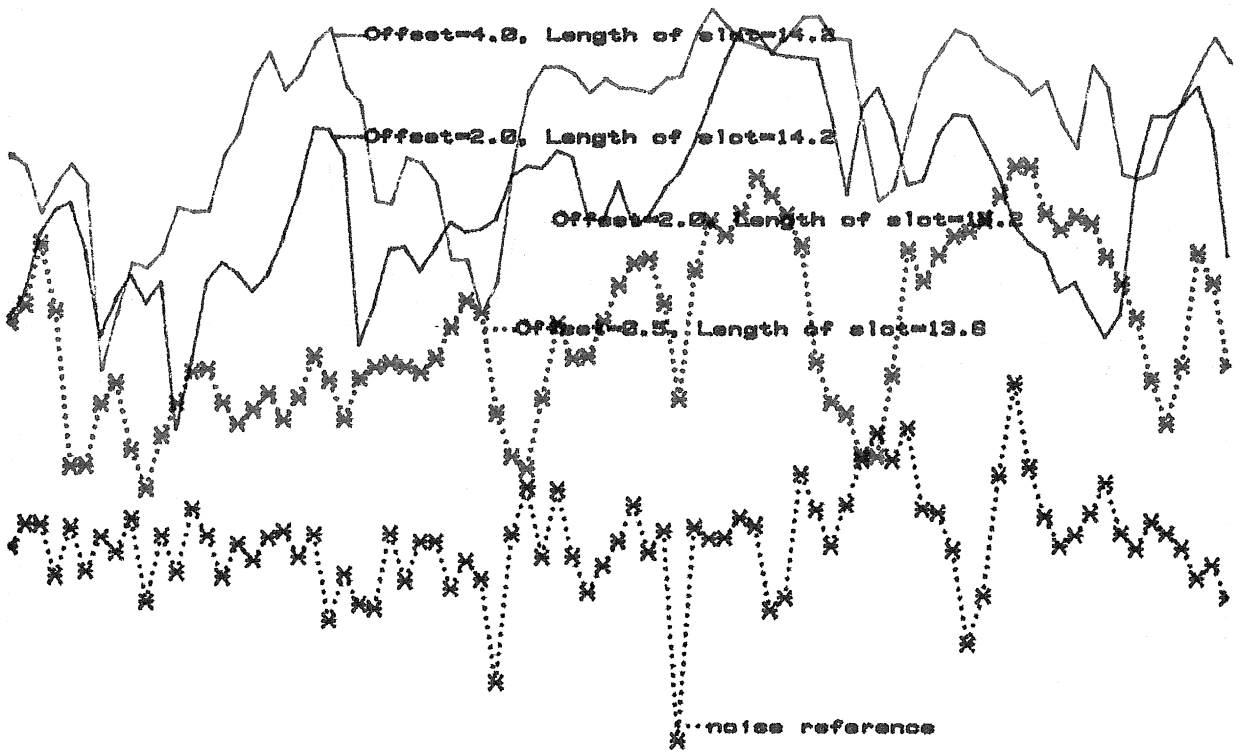

4.14

ALL OFFSET AND LENGTH DIMENSIONS IN MM.

Fig. 4.14. Figure showing the comparisons of the variation of the main lobe power received with the frequency for the offset and the length of slots settings of Figs. 4.4, 4.7, 4.9 and 4.11.

Graphstar

the most evident in Fig. 4.14 where four prominent main lobes have been plotted simultaneously.

- It is expected that as the slots lengths are increased, the main lobes shift in frequency. In the plotted graphs, as they are plotted with frequency on the X-axis, the resul would have become evident with the left shift of the best main lobes. However, no such phenomenon was observed.
- Though the side radiation has increased with increasing offset, its increase is not as marked as for the main lobe. This pattern gives an indication that the suppression of the parallel plate guide mode may be taking place.

3. *Side radiation.* Figs. 4.4—4.12 depict the side radiation patterns of various settings of the experiment. Fig. 4.15 depicts chosen four out of the above for a clearer comparison.
   - When we study Figs. 4.9 and 4.10, where offsets are 4.0mm and 4.5mm for slot lengths of 14.2mm, it is found that wherever the structure resonates, side radiation level dips drastically but the main lobe is hardly affected. This is the most prominent at 10.7 GHz.
   - Similarly, in Fig. 4.11, with offset of 4.5mm and length of 15.2mm, this pattern is repeated and suppression is the most prominent. At lower offsets, the prominence is reduced but is nevertheless present.
4. On studying figs. 4.6, 4.7, 4.8, 4.9 and 4.10, where the difference is only in feed point offset, it is seen that the S_{11} characteristics are greatly affected while main lobe initially becomes better and then almost constant. In side radiation pattern, the dips at resonance generally improve with the offset.

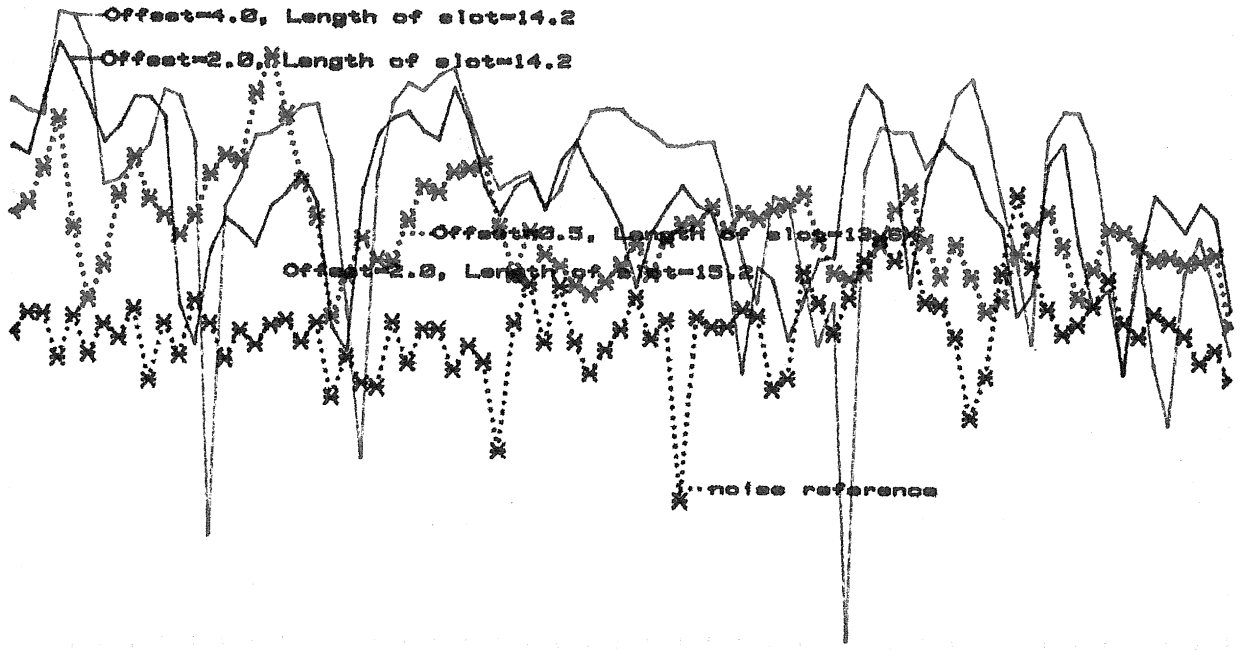

4.15

ALL OFFSET AND LENGTH DIMENSIONS IN MM.

Fig. 4.15. Figure showing the comparisons of the variation of the side radiations received with the frequency for the offset and the length of slots settings of Figs. 4.4, 4.7, 4.9 and 4.11.

Graphstar

4.7 Conclusion

- It is thus concluded that the method for suppression of the parallel plate guide mode in a stripline structure is quite effective. However, in the conducted study, the suppression occurs at a point about 7% off from the design frequency.

- No appreciable suppression takes place if the offset is kept at the calculated values. In this experimental study, it was found that the suppression improved as the offset was increased upto about eight times the calculated value. Due to practical limitations of design, an offset more than this could not be checked. Thus, there seems to be some serious flaw in the calculations by the available formulae in this case.

- Another reason may be that the parallel plate guide mode (internal side radiation) alter the active impedance of the slots to such a great degree that the offset calculations by available formulae cease to hold good.

- In order to fabricate a stripline-fed slot pair , it is therefore required to carry out a rigorous analysis so that the exact reason for the above deviation can be found out and the calculations adjusted suitably.

Chapter 5

Conclusion

In this study, the main objective was to design and conduct an experimental study of a structure for stripline–fed slot array which would be able to overcome the problem of parallel plate guide mode . After studying and enumerating the drawbacks of methods like shorting pins, metallized cavities and shorting holes which are currently being used, it was decided to fabricate and experimentally study two structures to explore their feasibility.

The first structure, namely, cavity–backed stripline–fed slot was fabricated using a rectangular cavity with variable depths so as to be able to plot curves for varying cavity depths and then study the emerging patterns. However, nothing of much consequence emerged from this study. This may be attributed to a multiplicity of transitions and change of mediums which were not taken into account in the design as also a lack of understanding of the fields in such a structure.

The second structure, namely, stripline–fed slot pair, gave much more promising results. As the offset of the feedline from the edge of the slots was increased towards the centre of the slots, a clear suppression of the parallel plate guide mode could be seen. The only problem was that it occurred at a frequency approximately 7% more

than the design fequency. This could not be corrected even by increasing the slot lengths. Also, the offset calculations done using available formulae from [18] were wide off the mark.

Thus, to conclude, the second structure of a stripline–fed slot pair *does hold a lot of promise* as far as suppression of parallel plate guide mode is concerned. However, a lot of work still needs to be done for an accurate analysis of the fields prevailing in this structure. Then it may be possible to get the suppression at the design frequency.

References

[1] E.G. Fubini, J.A. McDonough and R.G. Malech, "Stripline radiators," *IRE Conv. Rec.*, part 1, pp. 51-55, 1955.

[2] J.A. McDonough, R.G. Malech and J. Kowalsky, " Recent developments in the study of printed antennas," *IRE Conv. Rec.*, part 1, pp. 173-176, 1957.

[3] A.A. Oliner, "The radiation conductance of a series slot in strip transmission line," *IRE Conv. Rec.*, vol. 2, part 8, pp. 89-90, 1954.

[4] D.J. Sommers, "Slot arrays employing photo-etched tri-plate transmission lines," *IRE Trans. Microwave Theory Tech.*, vol. MTT-3, pp. 157-162, Mar. 1955.

[5] R.W. Breithaupt, "Conductance data for offset series slots in stripline," *IEEE Trans. Microwave Theory Tech.*, vol. MTT-16, pp. 969-970, Nov. 1968.

[6] Y. Yoshimura, "A microwave line slot antenna," *IEEE Trans. Microwave Theory Tech.*, vol. MTT-20, pp. 760-762, Nov. 1972.

[7] H.G. Ottman, "Electromagnetically coupled microstrip dipole antenna elements," *presented at Proc. 8th European Microwave Conference*, Paris, France, Sep. 1978.

[8] D.A. Heubner, "An electrically small microstrip dipole planar array," *presented at Proc. workshop on Printed Circuit Antenna Tech.*, New Mexico, Oct. 1979.

[9] R.S. Elliott and R.J. Stern, "The design of microstrip dipole arrays including mutual coupling , PartI : Theory and PartII : Experiment," *IEEE Trans. Antennas Propagat.*, vol. AP-29, pp. 135–140, Sept. 1981.

[10] Pyong K. Park and R.S. Elliott, "Design of collinear longitudinal slot arrays fed by a boxed stripline," *IEEE Trans. Antennas Propagat.*, vol. AP-29, pp.135–140, Jan. 1981.

[11] B.N. Das and K.K. Joshi, "Impedance of a radiating slot in the ground plane of a microstripline," *IEEE Trans. Antennas Propagat.*, vol. AP-30, pp. 922–926, Sept. 1982.

[12] Reuven Shavit and R.S. Elliott, "Design of transverse slot arrays fed by a boxed stripline," *IEEE Trans. Antennas Propagat.*, vol. AP-31, pp. 545–552, Jul. 1983.

[13] B.N. Das and K.V.S.V.R. Prasad, "Impedance of a transverse slot in the ground plane of an offset stripline," *IEEE Trans. Antennas Propagat.*, vol. AP-32, pp. 1245–48, Nov. 1984.

[14] R.R. Robertson and R.S. Elliott, "Design of transverse slot arrays fed by the meandering strip of a boxed stripline," *IEEE Trans. Antennas Propagat.*, vol. AP-35, pp. 252–255, Mar. 1987.

[15] Robert J. Mailloux, "On the use of metallized cavities in printed slot arrays with dielectric substrates," *IEEE Trans. Antennas Propagat.*, vol. AP-35, pp. 477–487, May 1987.

[16] W.L. Weeks, "Antenna engineering," McGraw Hill Book Company Inc., New Delhi, 1974.

[17] D.M. Pozar, N.K. Das, B.N. Das and K.K. Joshi, "Comments on impedance of a radiating slot in the ground plane of a microstrip line," *IEEE Trans. Antennas Propagat.*, vol. AP-34, pp. 958–959, Jul. 1986.

[18] R.S. Elliott, "Antenna theory and design," *Prentice-Hall*, New Delhi, 1985.

[19] E.C. Jordan and K.C. Balmain, "Electromagnetic waves and radiating systems, 2nd Ed.," *Prentice-Hall*, N.J., pp. 540–547, 1968.

[20] C.T. Tai, "Characteristics of linear antenna elements, ed. H. Jasik," *McGraw-Hill*, N.Y., chap. 3, 1961.

[21] H.G. Booker, "Slot aerials and their relation to complementary wire aerials (Babinet's principle)," *JIEE, Part IIIA*, pp. 620–626, 1946.

[22] H.M. Altschuler and A.A. Oliner, "Discontinuities in the center conductor of symmetric strip transmission line," *IRE Trans. Microwave Theory Tech.*, vol. MTT-8, pp. 328–339, May 1960.